Development and application of the thermodynamic database PRODATA dedicated to the monitoring of mining activities from exploration to remediation

Pascal E. Reiller, Michaël Descostes

Development and Application of the Thermodynamic Database PRODATA Dedicated to the Monitoring of Mining Activities from Exploration to Remediation.

Pascal E. Reiller[a,*] and Michaël Descostes[b]

[a]Den – Service d'Études Analytiques et de Réactivité des Surfaces (SEARS), CEA, Université Paris-Saclay, F-91191 Gif-sur-Yvette, France.

[b]ORANO Group Mining R&D Dpt, 125 avenue de Paris, F-92320 Châtillon, France

* corresponding author : pascal.reiller@cea.fr

Abstract

A growing demand exists on the monitoring of both uranium mining activities and their environmental impacts. In order to help understanding and modelling both these aspects, a thermodynamic database dedicated to uranium mining activities is built: the PRODATA database. Relevant species and phases for uranium and radium are chosen from existing compilations of data, complemented with important missing data for the application to mining activities and environmental monitoring. Important major anions and cations chemistry are included, as well as secondary pollutants such as arsenic, lead or nickel. Applications of the PRODATA extracted database file for PhreeqC to theoretical speciation calculations of uranium and radium for actual water compositions — either linked to uranium mining activities, or under monitoring for environmental survey — are presented. Wider applications to other available water compositions from different geochemical concepts are also tested. For the tested cases, the major radium and uranium species obtained using PRODATA are compared with other available thermodynamic database (Thermochimie, LLNL, Wateq4f, Minteq, PSI/NAGRA). The choice of the database file — and of the ionic strength correction — can strongly impact the final speciation results. Sulphate complexes of radium and uranium are of particular importance in mining exploitation context, and carbonate uranium complexes — particularly $Ca_nUO_2(CO_3)_3^{(4-2n)-}$ complexes — are crucial for environmental monitoring. The latter complexes are key species for the aqueous speciation of uranium even in reducing environment where U(IV) low solubility usually governs uranium mobility.

1. Introduction

Evaluation of environmental impact of anthropic activities, particularly of mining activities, must be considered before any industrial project development. One of the approaches currently developed relies on predictive reactive transport modelling. Such strategy requires, on the one hand, a thorough description of the physico-chemical reactions that govern the mobility of contaminants of concern and, on the other hand, their couplings in order to better constrain the studied system. These approaches allow testing several evolution scenarii on space and time scales beyond the ones probed by laboratory and field experiments (Steefel et al., 2015). This is particularly true for: (i) mining and nuclear industries (Zhu et al., 2001; Curtis et al., 2006) including the management of legacy sites (Drozdzak et al., 2016; Husson et al., 2019); (ii) uranium in the framework of long-term safety assessment of radioactive waste repositories (van der Lee et al., 2003; Montarnal et al., 2007; Claret et al., 2018; Mühr-Ebert et al., 2018); (iii) management of polluted soils and aquifers inherited from the use of depleted uranium from armor-piercing ammunition (Chen and Yiacoumi, 2002; Mitsakou et al., 2003); (iv) assessment of the ecotoxicological impact of uranium (Paredes et al., 2016, 2018; Husson et al., 2019; Lartigue et al., submitted). One may also use such an approach for mining exploration, optimizing mining operations — especially in the case of In Situ Recovery (ISR) mines (Johnson and Tutu, 2016; Lagneau et al., 2019) —, and remediation (Yabusaki et al., 2007).

Uranium is considered as a trace element that is showing a complex aqueous chemistry, especially in natural environments. Its mobility is generally governed by pH and redox, the presence of inorganic — e.g., CO_3^{2-}, SO_4^{2-}, PO_4^{3-} (Guillaumont et al., 2003) — and

55 organic ligands (Hummel et al., 2005), but also adsorption reactions at the mineral water
56 interfaces — see Lartigue et al. (submitted) and references therein. Hence, assessing and
57 understanding the geochemical mechanisms controlling the mobility of uranium in the
58 environment requires also the consideration of the other major elements chemical
59 properties, which are often observed at higher significant concentrations.

60 The environmental footprint of uranium mines is driven, on the one hand, by the mining
61 extraction process, and, on the other hand, by the composition of the treated ore. The
62 extraction processes generally involve highly concentrated and oxidizing solutions — in
63 sulphuric acid or under alkaline conditions — in order to increase uranium solubility. In
64 addition to ^{226}Ra — one of the main radioactive decay products of ^{238}U —, the ores are
65 generally associated to other metals (e.g., Ni, Fe, Mo, Cu…) and metalloids (e.g., As, Se…).
66 These elements are showing different geochemical behaviours than U, and may become
67 in turn (secondary) contaminants.

68 The geochemical behaviour of ^{226}Ra is particular. Through its radioactive half-life (1 600
69 years) and its high specific activity (36.6 GBq g^{-1}), ^{226}Ra is always observed at elementary
70 concentrations drastically lower than uranium. As an illustration, for a uranium ore older
71 than 1 My, with an average U content of 1‰ (*ca.* 12 500 Bq kg^{-1}), the secular equilibrium
72 will lead to a hypothetical ^{226}Ra concentration of 342 ppt. The migration of ^{226}Ra in the
73 environment is mainly governed by adsorption reactions (see e.g., Sajih et al., 2014;
74 Reinoso-Maset and Ly, 2016; Robin et al., 2017; Bordelet et al., 2018), coprecipitation
75 through solid solution formation with other alkaline earth sulphate minerals (Curti et al.,
76 2010; Lestini et al., 2019), and carbonate bearing minerals (Jones et al., 2011).

77 The description of the physico-chemical reactions involved, directly or indirectly, in the
78 fate of contaminants is usually gathered in a thermodynamic database. It includes redox
79 and aqueous complexation formation equilibria, dissolution or formation of solid or
80 gaseous phases; sometimes, coprecipitation or adsorption reactions are also included. To
81 perform the calculation on these intricate systems, several modelling codes are available,
82 from aqueous speciation calculation to reactive transport, even if this approach has
83 inherent limitations (Nordstrom, 1996), particularly concerning uncertainties (Emrén et
84 al., 1999; Ekberg and Ödegaard-Jensen, 2011; May and Filella, 2011)

85 Currently, ORANO Mining, the historic French uranium mining company (former AREVA
86 Mines and Cogema, https://www.orano.group/en/expertise/from-exploration-to-
87 recycling/leading-uranium-producer), has to answer to different national regulators and
88 nuclear safety agencies for the exploration, exploitation, and remediation of its sites. This
89 includes the building of Safety Cases, applying Safety Assessment processes, which
90 require evaluation of the chemistry of uranium, radium, and other eventual secondary
91 pollutants, in different contexts, including speciation and transport. Different softwares
92 are usually needed to attain these objectives, which provided databases are generally not
93 built around the same core of data. To provide robust cases, there is a need to have a
94 common database for the different softwares used to perform the calculations. ORANO
95 Mining is using widely available speciation codes, i.e. PhreeqC (Parkhurst and Appelo,
96 1999, 2013), CHESS (http://chess.geosciences.mines-paristech.fr/?set_language=en),
97 and the Geochemists' WorkBench (GWB, http://www.gwb.com), with which
98 thermodynamic database files are provided. However, a thermodynamic database that
99 can be used with several codes, and can be exploited in monitoring of mining activities, is

seldom found. Besides, thermodynamic databases provided with the different modelling codes do not systematically share either the same thermodynamic data, the same traceability, or the same completeness (Hummel et al., 2019). Direct comparison between modelling codes' results, but also between studied cases, may therefore be limited.

Uranium is the central element of the nuclear fuel cycle. Its thermodynamic properties have been the subject of a large body of work. The data selections that are subject of the largest consensus have been commissioned by the Thermochemical DataBase (TDB) project from the Nuclear Energy Agency (NEA) within the Organization for the Economic Co-operation and Development (OECD) (Wanner, 1988; Mompeán and Wanner, 2003; Ragoussi and Brassinnes, 2015). The selection is including inorganic (Grenthe et al., 1992; Guillaumont et al., 2003) and selected organic complexes (Hummel et al., 2005) — a PhreeqC database file has been made available recently (Martinez et al., 2019). The selection criteria being rather strict, it is inevitable that some data are rejected, and cannot be used as is to perform calculations in relevant media for mining activities and environmental monitoring. A recent study suggests that database files that are sit on the NEA-OECD database selection can be more likely recommended to estimate uranium speciation (Wang et al., 2019), but effectively needed some implementations from other sources, even if traceability issues may appear (Hummel et al., 2019).

Despite of the great interest in the monitoring of mining activities, radium has not been the subject of the same attention. Nevertheless, some data are available, and have sometimes been included in databases.

To perform relevant speciation calculation in actual situations, the database used should be containing the relevant chemical equilibria and species predominant in the system to describe the geochemistry of the site, and should also be as consistent as possible. In addition to uranium, the TDB project from NEA-OECD has commissioned reviews on elements relevant for the management of radioactive wastes that can be directly implemented in a database (e.g., Brown et al., 2005; Gamsjäger et al., 2005; Olin et al., 2005; Rand et al., 2009; Lemire et al., 2013). From the strict definition of the selection criteria of the NEA-OECD selection, it can be understood that complementary data must be implemented either on already reviewed elements, or on elements that are necessary for natural or mining systems, such as e.g. Ca, Mg, Al or Si.

Some thermodynamic database files provided with softwares are containing a large body of data on several complexes and phases. But the data within these database files are not always easy to trace, as they are necessarily in the NEA-OECD reviews. There is a pressing demand from nuclear safety authorities to provide evidence that the data used to evaluate a speciation calculation are traceable and retrievable, which if achieved provide a further confidence in the evaluation of a safety case.

From these constraints and legal obligations, there is a need for the building of a thermodynamic database dedicated to uranium mining activities from exploration to remediation: the PRODATA database. This database was thought as a tool in which thermodynamic data (constants and functions) relevant for mining activities and environmental monitoring can be compiled, and database files for the different speciation codes can be exported on demand. Once available, the applicability of the database to specific cases directly linked to uranium mining activities must be verified. These cases

must cover a wide range of applications on uranium and radium: (i) historic impacted sites that either will be submitted to remediation processes, or are in course of remediation (i.e., legacy sites); (ii) sites where mining operations are currently in exploitation; and (iii) sites that are under exploration for future exploitation. These three steps representing the life cycle of a mining site in general, and of uranium mining in particular.

To offer a more complete view on the application fields of PRODATA, we have selected a range of water compositions at the boundaries of the uranium mining operations: (i) waters that are not yet impacted either by mining operation or by the nuclear fuel cycle in general; (ii) waters that are impacted by different parts of the nuclear fuel cycle including radioactive waste management; and (iii) waters that are naturally impacted by noticeable natural uranium concentrations. The speciation of these waters will be done on uranium — either using the available amount or in equilibrium with a relevant phase — and radium — if available in the composition.

The database file for speciation code PhreeqC extracted from PRODATA will be used to perform uranium and radium speciation calculations for these different water compositions. The results will be compared with other database files that are either provided in the PhreeqC package or provided by the developers of the database. General comportment of uranium and radium will be discussed for the different cases studied. This work can be seen as a benchmark of the PRODATA database, but should not be viewed as a qualitative comparison with the other databases, which are for some of them not developed specifically for the application to monitoring of uranium mining activities.

2. Construction of the database and general framework of the modelling exercise.

2.1. Construction of the database

2.1.1. Database formats required for speciation codes

The specific needs from speciation modelling for Orano Mining imply the use of several speciation softwares, i.e. PhreeqC, CHESS, and GWB. As written earlier, several database files are provided with these softwares, but none of them is available for the three codes, at least a database file that would cover the need for mining and environmental monitoring. The need to have the same database in order to obtain coherent calculations using the three speciation codes have been clearly identified. If this work is focused on the PhreeqC database file, a companion study using the CHESS database file is also available in this volume (Lartigue et al., submitted).

2.1.2. Requirement imposed by the extraction of database files to several codes

2.1.2.1. General constraints

Building a database that can be extracted to, and used by, several speciation or transport codes imposes a certain amount of constraints. All of the codes have different ways of formatting the database files, but some commonalities are existing.

The main constraint comes from the definition of the basic species and how equilibria are written. PhreeqC imposes the definition of MASTER species (SOLUTION_MASTER_SPECIES keyword), gives the possibility to define secondary redox species, and then allows the definition of complexes in a very flexible way. The more illustrative example is the definition of phosphate complexes, where complexes relative to PO_4^{3-}, HPO_4^{2-}, $H_2PO_4^-$, or $H_3PO_4(aq)$ can coexist as long as all equilibria between species

are defined in the database. In Guillaumont et al. (2003) the $\log_{10}\beta°$ values of the $UO_2PO_4^-$ and $UO_2HPO_4(aq)$ complexes are defined relative to PO_4^{3-} and HPO_4^{2-}, respectively, as

$$PO_4^{3-} + UO_2^{2+} \rightleftarrows UO_2PO_4^- \qquad \log_{10}\beta° = 12.23 \pm 0.15$$

and

$$HPO_4^{2-} + UO_2^{2+} \rightleftarrows UO_2HPO_4(aq) \quad \log_{10}\beta° = 7.24 \pm 0.26$$

that can coexist in a PhreeqC database file, associated with the acidity constants for phosphate species.

These definitions will not be recognized either by CHESS or GWB that impose the definition of a single ligand species implied in reactions beyond the redox definition. Depending on the choice of the "basis-species" definition in CHESS or GWB, preceding equilibria must be written relative to only one phosphate species.

Hence, for the sake of adaptability, a common choice of a single basic species for a ligand is done, and the $\log_{10}\beta°$ values are recalculated from the stoichiometry of the reactions, and using the thermodynamic functions, whenever available.

In PRODATA, the choice of PO_4^{3-} is done, and for the $UO_2HPO_4(aq)$ complex it comes,

$$PO_4^{3-} + H^+ + UO_2^{2+} \rightleftarrows UO_2HPO_4(aq) \qquad \log_{10}\beta° = 19.59 \pm 0.26$$

which assures the compatibility for the three codes. The definition relative to sulphate and carbonate complexes are done relative to SO_4^{2-} and CO_3^{2-} — even if the swap between CO_3^{2-} and HCO_3^- is possible.

2.1.2.2. Definition of redox equilibria

Another constraint is the definition of redox equilibria. If all the redox equilibria can be defined relative to the electron in PhreeqC, they have to be defined relative to O_2(aq) in CHESS and GWB — even if GWB requires the definition of e^-. But in PhreeqC, both the oxidation of H_2O and reduction of H^+ have to be defined relative to e^-. The choice of the definitions of the other redox equilibria relative to O_2(aq) are then done for the sake of compatibility of the different equilibrium reactions and export to CHESS and GWB.

As for the swap between CO_3^{2-} and HCO_3^-, some redox swaps are possible, as e.g., SO_4^{2-}/HS^-, SeO_4^{2-}/HSe^-, $AsO_4^{3-}/H_2AsO_3^-$, Fe^{3+}/Fe^{2+}, MnO_4^-/Mn^{2+}, or UO_2^{2+}/U^{4+}.

2.1.2.3. Use of metastable species

The particular cases of metastable species is particularly difficult to handle in thermodynamically based speciation codes — particularly in PhreeqC, CHESS, and GWB. The most illustrative example is the formation of perchlorate ion ClO_4^-, which is metastable in water, but is the basis of the complexation studies in indifferent background electrolyte media. The other would be the account of organic ligands that are thermodynamically metastable in the water stability domain. The most convenient way to handle this is through the definition of independent species to circumvent thermodynamically driven decomposition of molecules during the calculation, which would "remove" a ligand from, or change a background electrolyte in, the solution. Both PhreeqC and CHESS allow defining these kinds of species, but the constraints of GWB *basis-species,* made of elements with only two letters, is more difficult. Hence, the definition of species that are not composed of elements from the periodic table is done in

229 both PhreeqC and CHESS — e.g., for PhreeqC, a species name “Perchlorate-” for ClO_4^-,
230 “Thiocyanate-” for SCN^-, or “Selenocyanate-” for $SeCN^-$ —, but is not yet available in GWB
231 version of PRODATA. Another possibility would be to handle the metastability through
232 kinetic reactions. But a kinetic database for uranium speciation, or for other elements, is
233 not available. It is noteworthy that other softwares allow validating or devalidating
234 specific reactions (e.g., CHNOSZ http://chnosz.net/) to handle metastability.

235 2.1.3. Physical constants and atomic weight of the elements

236 The physical constants are the one used in the NEA-OECD database (Guillaumont et al.,
237 2003), and the atomic weight of the elements, and eventual isotopes, are taken from
238 Wieser (2006).

239 2.1.4. Thermodynamic Data

240 From the constraints already exposed (vide ante), whenever possible, the thermodynamic
241 functions of formation on the molal scale of the species (i.e., $\Delta_f G_m^o$, $\Delta_f H_m^o$, $S_{f,m}^o$, and $C_{p,m}^o$)
242 are used within the database. The thermodynamic functions of reaction (i.e., $\Delta_r G_m^o$, $\Delta_r H_m^o$)
243 are calculated from the formation reaction of a species, or the dissolution reaction of a
244 phase, then the thermodynamic constant at 25°C is calculated.

$$\log_{10} K° = -\frac{\Delta_r G_m^o}{RT \ln(10)} \quad (1)$$

245 The uncertainties for the formation or dissolution of species are calculated from the
246 propagation of errors and are given as comments.

247 At other temperature, the $\log_{10} K$(T) are calculated from

$$\log_{10}K°(T) = \log_{10}K°(T_0) - \frac{\Delta_r H_m^o(T_0)}{RT\ln(10)}\left(\frac{1}{T} - \frac{1}{T_0}\right) \quad (2)$$

neglecting the effect of $\Delta_r C_{p,m}^o$ in a first approximation, which is reasonable is view of the application domain of this database.

Due to the necessary heterogeneous provenance of the data included in PRODATA, the homogeneity of the thermodynamic functions of formation is not assured *a priori*. Consistency checks, as done otherwise (Wagman et al., 1982; Guillaumont et al., 2003) are not assured for the moment. Some sources are providing thermodynamic functions (Wagman et al., 1982; Cox et al., 1989; Robie and Hemingway, 1995; Chase, 1998), others are providing thermodynamic constants (Smith et al., 2004), and other give both types of data (Grenthe et al., 1992; Guillaumont et al., 2003; Brown and Ekberg, 2016). It is also noteworthy to recall that not all these databases do share the same level of traceability (Hummel et al., 2019).

The primary data for the characterisation of a reaction is the $\log_{10}K°$ value, from which $\Delta_r G_m^o$ is calculated (eq. 1). Then $\Delta_f G_m^o$ is obtained using other Gibbs energies of formation from the implied reactants and products. In PRODATA exported database files, as $\log_{10}K°$ are calculated from the $\Delta_r G_m^o$ — with the exception detailed later (vide infra) — it was decided, whenever possible, to recalculate the $\Delta_f G_m^o$ of the species. This implies an essential choice on the origin of the Gibbs energies of formation. This is surely not a consistency check, but to our vision this allows limiting some inconsistency problems, as those evidenced otherwise (Endrizzi et al., 2016).

As it will be detailed later in the text, the choice of the works from CODATA (Cox et al., 1989) was made because it forms the foundation of the thermodynamic data selection for uranium by the TDB Project from NEA-OECD. As an example, we will explain the particular case of copper, which data are barely available with the NEA-OECD selection of data, but can be important for mining and environmental monitoring (Cretaz et al., 2013). The thermodynamic functions of formation for Cu^{2+} are available in NEA-OECD (Guillaumont et al., 2003) — selected from CODATA (Cox et al., 1989) —, but the data from $Cu(SO_4)(aq)$ are available in the United States National Bureau of Standard (NBS) thermodynamic selection of data (Wagman et al., 1982) with slightly different $\Delta_f G_m^o$ for both Cu^{2+} and SO_4^{2-}. Within PRODATA, the thermodynamic functions of formation for $Cu(SO_4)(aq)$ are calculated as shown, taking $\Delta_f G_m^o$ as an example.

$$Cu^{2+} + SO_4^{2-} \rightleftarrows Cu(SO_4)(aq)$$

$$\begin{aligned}\Delta_r G^o_{m,Wagman} &= \Delta_f G^o_{m,Wagman}\big(Cu(SO_4)(aq)\big) - \Delta_f G^o_{m,Wagman}(Cu^{2+}) \\ &\quad - \Delta_f G^o_{m,Wagman}(SO_4^{2-}) \qquad (3)\\ \Delta_r G^o_{m,Wagman} &= -692.18 - (65.49 - 744.53) = -13.40\ \text{kJ.mol}^{-1}\end{aligned}$$

$$\begin{aligned}&\Delta_f G^o_{m,Prodata}\big(Cu(SO_4)(aq)\big) \\ &\quad = \Delta_r G^o_{m,Wagman} + \Delta_f G^o_{m,Prodata}(Cu^{2+}) + \Delta_f G^o_{m,Prodata}(SO_4^{2-}) \qquad (4)\\ &\Delta_f G^o_{m,Prodata}\big(Cu(SO_4)(aq)\big) = -13.40 + 65.046 - 744.004\end{aligned}$$

$$\Delta_f G^o_{m,Prodata}\big(Cu(SO_4)(aq)\big) = -692.098\ \text{kJ.mol}^{-1}$$

Through this calculation, the obtained $\log_{10} K° = 2.30$ in PRODATA is coherent with its initial value obtained using Wagman et al. (1982).

Not assuring this conversion can lead to great discrepancies and inconsistencies, if origins of the data are not controlled. As an example, one can check the differences between the published solubility constants of the phases from the liebigite group — $^{I}M_{2n}\,^{II}M_{m}\,^{II}M'_{(2-n-m)}UO_2(CO_3)_3 : xH_2O$ where ^{I}M is an alkaline metal, and ^{II}M and $^{II}M'$ are alkaline earth metals — and those recalculated using improper thermodynamic functions — see analyses and discussion in Endrizzi et al. (2016).

In some cases, the thermodynamic functions of formation may not be available — e.g., for amorphous solids, which hydration numbers are not known — or for species whose extrapolation of formation constant to infinite dilution is not yet assessed. In these particular cases, the $\log_{10}K°$ for the formation or dissolution reactions is given explicitly in a different section within the respective keyword section. If the $\Delta_r H_m^o$ is available, then it is either exported to the PhreeqC database file, or the $\log_{10}K(T)$ are calculated from eq. 2 for CHESS and GWB database files.

All the data within the database are traced to the original publications, or duly commented if the origin is at stake. It is the case for some clayey phases included in other software databases, which are nice-to-have data, but not directly or easily traceable.

2.1.5. Uncertainties

In the majority of cases, speciation softwares do not offer uncertainty estimations of the final results, with noticeable exceptions (Ödegaard-Jensen et al., 2004; Ekberg and Ödegaard-Jensen, 2011; MCPhreeqc, 2011). When the uncertainties of the thermodynamic functions and constants are given — e.g., Cox et al. (1989) and Guillaumont et al. (2003) —, they are directly implemented in PRODATA. The other

available uncertainties are re-estimated by propagation of errors when $\Delta_f G^o_{m,Prodata}$ are recalculated.

In the case of $Cu(SO_4)(aq)$, the uncertainty given by the NBS (Wagman et al., 1982) is between 8 to 80 times the last digit of the data. Choosing 8 times, it comes,

$$\sigma\left(\Delta_f G^o_{m,Prodata}\left(Cu(SO_4)(aq)\right)\right)^2 = \sigma\left(\Delta_r G^o_{m,Wagman}\right)^2 + \sigma\left(\Delta_f G^o_{m,Prodata}(Cu^{2+})\right)^2 + \sigma\left(\Delta_f G^o_{m,Prodata}(SO_4^{2-})\right)^2 \quad (5)$$

$$\sigma\left(\Delta_f G^o_{m,Prodata}\left(Cu(SO_4)(aq)\right)\right)^2 = (0.408)^2 + (1.557)^2 + (0.418)^2 \quad (6)$$

$$\sigma\left(\Delta_f G^o_{m,Prodata}\left(Cu(SO_4)(aq)\right)\right) = 1.663\ \text{kJ.mol}^{-1} \quad (7)$$

which finally gives

$$\Delta_f G^o_{m,Prodata}\left(Cu(SO_4)(aq)\right) = -(692.098 \pm 1.663)\ \text{kJ.mol}^{-1}$$

and

$$\log_{10} K° = 2.30 \pm 0.07$$

2.1.6. Deviation from ideality – Ionic strength correction

Ionic strength correction can be a serious issue to tackle — see Grenthe et al. (1997) for detailed analysis. Concerning the monitoring of mining activity, impacted natural water can show a large span of salinity, and rather high concentrations of sulphuric acid are used to extract the uranium ore.

The theoretical calculation of speciation cannot only rely on Davies (1962) relationship that allow calculating the mean activity coefficient of a species j of charge z_j,

$$\log_{10}\gamma^{\pm} = -z_j^2 A\left(\frac{\sqrt{I_m}}{1+\sqrt{I_m}} - 0.3\, I_m\right) \quad (8)$$

where A is a temperature dependant constant (Helgeson and Kirkham, 1974; Grenthe et al., 1992; Guillaumont et al., 2003), and I_m is the ionic strength on the molal scale (mol kg_{water}^{-1}).

Furthermore, as several ions are forming the composition of water, the use of more advance relationship, as the one from e.g. Kielland (1937), does not allow calculating the global ionic strength influence of the mixture. In agreement with the selection from NEA-OECD (Grenthe et al., 1992; Grenthe and Puigdomènech, 1997; Guillaumont et al., 2003), and for ionic strength typically lower than 3 mol kg_{water}^{-1}, the specific ion interaction theory (SIT) can be used with PRODATA database when the ion specific parameters $\varepsilon(M^+, X^-)$ — M^+ and X^- being the cation and anion from the background electrolyte, respectively — are available or can be estimated for the j ion

$$\log_{10}\gamma_j = -\frac{z_j^2 A\sqrt{I_m}}{1+1.5\sqrt{I_m}} + \sum_k \varepsilon(j,k,I_m) \quad (9)$$

where *k* represented the opposite charged ion of the background electrolyte.

Based on the possibility to define metastable species (cf. § 2.1.2.3) all specific ion interaction coefficient relative to ClO_4^- in NEA-OECD selections are given relative to the Perchlorate- species in the PhreeqC database file from PRODATA.

The database file for PhreeqC is available for two different ionic strengths correction: Davies (1962), and specific interaction theory (SIT) calculations. The CHESS — as the one used in Lartigue et al. (submitted) — and GWB files are available for Debye-Hückel ionic strength corrections. In the following exercise, we will only discuss the use of the PhreeqC file exported from the PRODATA database for SIT calculations.

2.1.7. Oxygen and hydrogen

The basic properties of water are taken from CODATA (Cox et al., 1989) and NBS (Wagman et al., 1982). It is noteworthy that the thermodynamic data for the dissolution of $H_2(g)$ and $O_2(g)$ in water are not yet reported in the NEA-OECD selection. As these data are required for the building of the softwares' database files, the data for $H_2(aq)$ and $O_2(aq)$ were taken from NBS (Wagman et al., 1982).

2.1.8. Uranium

Uranium has received a consequent interest on its thermodynamic properties. A large body of work has been documented in the reviews commissioned by the Thermodynamic Database project of the NEA-OECD. Out of these volumes, uranium has been the subject of the first volume of the series (Grenthe et al., 1992), one addenda in the second volume (Silva et al., 1995), an update (Guillaumont et al., 2003), and the particular case of selected organic complexes (Hummel et al., 2005). All the fundamental thermodynamic functions on uranium from these reviews are coherent with the work from CODATA (Cox et al., 1989). The majority of the data recommended in these reviews are used in PRODATA, with the exception of data outside the scope of its application field — i.e., organic complexes, for the time being.

Some important phases were not selected in NEA-OECD compilations. For instance, phosphate (Muto, 1965; Van Haverbeke et al., 1996), or alkaline earth carbonate (Alwan and Williams, 1980; O'Brien and Williams, 1983). Nevertheless, the data from Muto (1965) on ningyoite ($CaU(PO_4)_2{:}\,2H_2O$), even not selected, were pointed out in NEA-OECD reviews (Grenthe et al., 1992; Guillaumont et al., 2003). The thermodynamic functions from Muto (1965) were adapted in PRODATA.

Concerning the hydrolysis of U(IV), the original selection in Grenthe et al. (1992) only selected $U(OH)^{3+}$ and $U(OH)_4(aq)$. The selection was modified in Guillaumont et al. (2003), but not other $U(OH)_n^{4-n}$ complexes were selected. In PRODATA, $U(OH)_2^{2+}$ and $U(OH)_3^{+}$ from Neck and Kim (2001), were added.

One of the major lack in the available data is the formation constants for $^{II}M_nUO_2(CO_3)_3^{(4-2n)-}$ complexes — with $^{II}M^{2+}$ being the alkaline earth cations. The first evidence of these complexes was in a seepage water from a uranium mine where Bernhard et al. (1996) — after the first data selection in Grenthe et al. (1992) — proposed the formation of $Ca_2UO_2(CO_3)_3(aq)$. Other authors confirmed the formation of $CaUO_2(CO_3)_3^{2-}$, $Ca_2UO_2(CO_3)_3(aq)$, and $MgUO_2(CO_3)_3^{2-}$ complexes (Kalmykov and Choppin, 2000; Bernhard et al., 2001; Dong and Brooks, 2006, 2008; Lee and Yun, 2013; Endrizzi and Rao, 2014; Lee et al., 2017), and their importance in theoretical speciation calculation was clearly shown (Kohler et al., 2004; Reiller et al., 2012; Vercouter et al., 2015; Neiva et al., 2019; Wang et al., 2019). The evidence of these species is particularly easy in time-resolved laser-induced luminescence as the triscarbonatouranyl(VI) complexes are the only ones to shown a hypsochromic shift relative to UO_2^{2+}. Endrizzi and

Rao (2014) has proposed $\Delta_f H_m^o$ values for $^{II}M_nUO_2(CO_3)_3^{(4-2n)-}$ complexes (Mg and Ca), which was included in PRODATA. Jo et al. (2019) proposed an analytical expression of the dependence of $\log_{10}\beta\left(Ca_nUO_2(CO_3)_3^{(4-2n)-}\right)$, which is not accounted in PRODATA due to its publication after the dead line fixed for the exercise (vide ante). These values are needed further confirmation.

Up to now, the NEA-OECD compilation of data does not recommend the use of these data because of a possible bias in extrapolation to zero ionic strength of the original data — see the discussion in Guillaumont et al. (2003) about Kalmykov and Choppin (2000). The use of the corresponding solids proposed by Alwan and Williams (1980) are not recommended either — see the discussion in Grenthe et al. (1992). Nevertheless, these complexes have been added to the PRODATA database in view of their importance in a wide range of carbonated waters conditions (Maher et al., 2013; Grivé et al., 2015). The results from the experiments from Dong and Brooks (2006) were chosen for $CaUO_2(CO_3)_3^{2-}$, $Ca_2UO_2(CO_3)_3(aq)$, $SrUO_2(CO_3)_3^{2-}$, $BaUO_2(CO_3)_3^{2-}$, and $Ba_2UO_2(CO_3)_3(aq)$. Concerning $MgUO_2(CO_3)_3^{2-}$ the extrapolation to infinite dilution proposed by Dong and Brooks (2008) was chosen, even if the SIT parameters can be viewed as too important compared to other divalent anions (Guillaumont et al., 2003). A discussion of this selection — in particular with the first proposition in Dong and Brooks (2006) —, in view of the speciation results, will be presented later (vide post).

For the solid phases, the problems in the data from Alwan and Williams (1980) identified in Grenthe et al. (1992), was later corrected by O'Brien and Williams (1983), and are included in PRODATA for scoping calculation. Endrizzi et al. (2016) proposed a re-

estimation of these solubility products in consistence with the formation of $^{II}M_nUO_2(CO_3)_3^{(4-2n)-}$ complexes in Endrizzi and Rao (2014). Even if they are known as alteration phases or uraninite (UO_2), in view of the high solubility of these phases, they should only be sparingly observed in monitoring of mining activities.

2.1.9. Radium

The thermodynamic functions and constants were taken from literature: Ra^{2+} and $RaNO_3^+$ were taken from NBS (Wagman et al., 1982). $RaOH^{2+}$, $RaCl^+$, $RaSO_4(aq)$, and $RaCO_3(aq)$ were taken from Langmuir and Riese (1985); $Ra(HCO_3)_n^{(2-n)+}$ were taken from Beneš et al. (1982).

For the solids, Ra(cr) and $Ra(NO_3)_2(s)$ are taken from NBS (Wagman et al., 1982), while $RaSO_4(s)$ and $RaCO_3(s)$ are taken from Langmuir and Riese (1985).

2.1.10. Auxiliary data

In order to perform the calculation needed for mining and environmental monitoring, a wide range of auxiliary data is needed, as uranium and radium are submitted to side complexation reactions.

2.1.10.1. Column VIIIA

Even if they are not necessary for the purpose of the database, noble gases — He, Ne, and Ar —, added as gases and dissolved species, are included in the PRODATA database. They could be used to fix a total pressure of inert gas over a solution.

417 *2.1.10.2. Column VIIA*

418 The halogens were mostly taken from CODATA, NBS, and NEA-OECD compilations
419 (Wagman et al., 1982; Cox et al., 1989; Guillaumont et al., 2003; Olin et al., 2005) and
420 complemented for I_3^- (Ramette and Sandford, 1965).

421 *2.1.10.3. Column VIA*

422 As already seen earlier, sulphur is an important auxiliary element for the monitoring of
423 mining operation, through sulphuric acid, particularly for ISR operations. Data for S^{2-},
424 $S_2O_3^{2-}$, SO_3^{2-}, and SO_4^{2-} were selected in Guillaumont et al. (2003), but they have been
425 complemented by the selected data from Chivot (2004) for S_n^{2-}, SO_2(aq), and other $S_nO_m^{2-}$.

426 Selenium, which isotope ^{79}Se is a fission product, is associated to uranium ores. It has been
427 the subject of an NEA-OECD volume (Olin et al., 2005) including uranium complexes,
428 which data are accounted for in PRODATA.

429 *2.1.10.4. Column V5*

430 Nitrogen and phosphorus species are taken from NBS (Wagman et al., 1982), CODATA
431 (Cox et al., 1989) and NEA-OECD (Guillaumont et al., 2003).

432 Arsenic can be an important contaminant that is accompanying uranium-mining activities
433 (Katsoyiannis et al., 2007; Neiva et al., 2019). The thermodynamic data selected during
434 the NEA-OECD compilation (Grenthe et al., 1992; Olin et al., 2005) are included in
435 PRODATA.

436 *2.1.10.5. Column IVA*

437 Due to its concentration in atmosphere, dissolution in water, and primordial importance
438 in the life cycle on Earth, carbon is an important auxiliary element to consider. Only
439 species from CO_2(g) dissolution in water (CO_2(aq), HCO_3^-, and CO_3^{2-}) and reduction to
440 methane (CH_4(g) and CH_4(aq)) are considered in PRODATA. Data from NBS (Wagman et
441 al., 1982), CODATA (Cox et al., 1989), and NEA-OECD (Guillaumont et al., 2003) are used.
442 The other organic compound or complexes from NBS (Wagman et al., 1982) or Hummel
443 et al. (2005) are not accounted for the time being.

444 Silicon is an important element in minerals, rock and sediment formation. The dissolved
445 silicate and polysilicate selected in NEA-OECD review are considered in PRODATA
446 (Guillaumont et al., 2003). Aluminum, iron (Hummel et al., 2002), and uranium
447 (Guillaumont et al., 2003) aqueous complexes are taken into account.

448 Only Si(cr) and quartz (SiO_2(cr)) are selected in the NEA-OECD data base (Guillaumont et
449 al., 2003). The SiO_2 solids are complemented by amorphous silica and chalcedony
450 (Nordstrom et al., 1990), coesite, cristobalite, quartz-alpha, quartz-beta, stishovite, and
451 tridymite (Fabrichnaya et al., 2004), and silicalite (Robie and Hemingway, 1995).

452 Lead is an important element as the end-result of the uranium decomposition chain. The
453 data were mainly selected from NBS (Wagman et al., 1982), CODATA (Cox et al., 1989),
454 Brown and Ekberg (2016), Sverjensky et al. (1997), Blanc et al. (2006) and Lothenbach et
455 al. (1999). For solids the compounds from NBS (Wagman et al., 1982) and CODATA (Cox
456 et al., 1989) are complemented by selenium compounds from NEA-OECD (Olin et al.,

2005), phosphate compounds (Nriagu, 1974), and hydroxocarbonate compounds (Taylor and Lopata, 1984)

2.1.10.6. Column IIIA

Aluminum is an important element as the counterpart of silicon in aluminosilicate minerals. The properties of aluminum have been proposed in NBS (Wagman et al., 1982) and CODATA (Cox et al., 1989), but more recent data were chosen for hydrolysis (Castet et al., 1993), fluoride (Nordstrom et al., 1990), and sulfate complexation (Tagirov and Schott, 2001).

Oxides (Robie and Hemingway, 1995), and sulfates (Helgeson et al., 1978; Wagman et al., 1982) were included. Several aluminosilicate are included (Helgeson et al., 1978; Robie and Hemingway, 1995; Gailhanou et al., 2012; Gailhanou et al., 2017). Some aluminosilicate selected in the GWB database were included in PRODATA even if it was not possible for the time being to identify the origin of the data. They are clearly marked as non-identified.

2.1.10.7. Column IIB

Zinc may be found in environmental mining context. Only Zn^{2+}, Zn(cr), ZnO, and some selenium compounds are available in NEA-OECD (Guillaumont et al., 2003; Olin et al., 2005). The hydrolysis is taken from Brown and Ekberg (2016) and Zhang and Muhammed (2001), the chloride complexes and $Zn(SO_4)(aq)$ and $Zn(SO_4)_2^{2-}$ from Powell et al. (2013), and the carbonate complexes from Smith et al. (2004).

The hydroxide is taken from Zhang and Muhammed (2001), sulphide phases are taken from Pankratz et al. (1987), sulphate and carbonate phases are from Robie and Hemingway (1995) — with the addition of $ZnSO_4:H_2O$ from Wateq4f (Ball and Nordstrom, 1991) —, and phosphate from Nriagu (1984).

2.1.10.8. Column IB

Copper can form very insoluble compounds with uranium (Cretaz et al., 2013). Even if data are available from NBS (Wagman et al., 1982), the hydrolysis data from Plyasunova et al. (1997), chloride from Wang et al. (1997), carbonate data from Smith et al. (2004) were chosen. The sulfate complex from NBS (Wagman et al., 1982) is included.

Silver Ag^+ ion, and the selenocyanate complex, is included in the NEA-OECD auxiliary data (Guillaumont et al., 2003; Olin et al., 2005). The selection is complemented by hydroxide (Bard et al., 1985), halogenide (Wagman et al., 1982; Bard et al., 1985), nitrate (Wagman et al., 1982), and carbonate (Sverjensky et al., 1997) complexes and solids.

2.1.10.9. Column VIIIB

Two nickel isotopes (^{59}Ni and ^{63}Ni) are activation products, and it is associated to uranium ores. Nickel has been the subject of a volume from NEA-OECD (Gamsjäger et al., 2005). Selenium compound were also selected (Olin et al., 2005).

Fe is ubiquitous on Earth. A first volume has been the subject of an NEA-OECD review (Lemire et al., 2013), and a selenium complex was selected (Olin et al., 2005). As this first NEA-OECD volume does not cover the entirety of the iron chemistry, other data were chosen to complement the selection for hydrolysis and chloride (Chivot, 2004), and

phosphate complexes (Nriagu, 1972b; Nriagu, 1972a). In addition to the solids selected in the NEA-OECD review (Lemire et al., 2013), hydroxide (Chivot, 2004), sulphur (Pankratz et al., 1987; Robie and Hemingway, 1995), and phosphorus (Nriagu, 1972b) are chosen. The Na-jarosite phase from LLNL database is included even if the origin were not identified up to now, but is identified as such.

2.1.10.10. Column VIIB

Manganese is often controlling the redox properties (Duro et al., 2000a). The thermodynamic data for redox and hydrolysis are chosen from Shock et al. (1997). Chloride and carbonate complexation are from Nordstrom et al. (1990), and fluoride are from Chandratillake et al. (1988) — these latter data are only added as $\log_{10}K°$ and not as $\Delta_f G_m^o$.

Solids from NBS (Wagman et al., 1982) and Robie and Hemingway (1995) are complemented by (oxo)hydroxides and carbonate (Nordstrom et al., 1990) and sulphur compounds (Pankratz et al., 1987; Dyrssen and Kremling, 1990).

2.1.10.11. Column VIB

Molybdenum has a rich chemistry, is often associated with uranium ores, and can be a secondary contaminant. The redox properties are mainly taken from Bard et al. (1985), and solids from Bard et al. (1985) and NBS (Wagman et al., 1982).

2.1.10.12. Column VB

Vanadium forms insoluble compounds with uranium. The redox chemistry is taken from Shock et al. (1997) and complemented by, NBS (Wagman et al., 1982), and Brown and Ekberg (2016). The solids are taken from Langmuir (1978), and NBS (Wagman et al., 1982).

2.1.10.13. Column IVB

Titanium and zirconium in the form of oxide minerals are often found in the environment. The data for titanium are taken from Brown and Ekberg (2016) for the aqueous species completed by solids from Bard et al. (1985), Robie and Hemingway (1995), and Pankratz et al. (1987). Zirconium has been the subject of a NEA-OECD review volume (Brown et al., 2005) due to its use as cladding for the nuclear fuel rods. The thermodynamic data and uncertainties recommended are included in PRODATA.

2.1.10.14. f-Transition Elements – Thorium

Apart uranium, thorium is the only *f*-transition element included up to now in PRODATA — other lanthanides or actinides are not of primary concern for the monitoring of mining activities. Thorium is part of the uranium radioactive decay chain. It has been the subject of one volume of the NEA-OECD (Rand et al., 2009). The thermodynamic data recommended, and uncertainties, are included in PRODATA.

534 *2.1.10.15. Column IIA*

535 Alkaline earth metals are important major cations to consider for environmental
536 monitoring of mining activities. They are implied in competition reactions for the main
537 environmental ligands, e.g. CO_3^{2-} through the formation of $^{II}M_nUO_2(CO_3)_3^{(4-2n)-}$
538 complexes (c.f. § 2.1.8), and SO_4^{2-} for the (co-)precipitation reaction of Ra in sulfate media
539 (Curti et al., 2010; Lestini et al., 2019).

540 The thermodynamic function for the free ions $^{II}M^{2+}$ are available in NEA-OECD
541 compilations (Guillaumont et al., 2003), but some important auxiliary data are not yet
542 available. Hydrolysis is taken from Palmer and Wesolowski (1997), Shock et al. (1997),
543 and Wagman et al. (1982). Fluoride and chloride complexes formation are taken from
544 Sverjensky et al. (1997). Sulfate complexes are taken from NBS (Wagman et al., 1982),
545 Yeatts and Marshall (1969), Reardon (1983), and Martell and Smith (1976). Nitrate
546 complexes are taken from NBS (Wagman et al., 1982). Carbonate complexes are taken
547 from Plummer and Busenberg (1982), Busenberg et al. (1984), and Busenberg and
548 Plummer (1986).

549 Some phases are selected in NEA-OECD compilations (Guillaumont et al., 2003), but they
550 do not allow calculating speciation in the conditions of mining activities monitoring.
551 Particularly, the hydroxide (Wagman et al., 1982; Chase, 1998; Felmy et al., 1998; Altmaier
552 et al., 2003), sulphur (Pankratz et al., 1987; Reardon and Armstrong, 1987; Robie and
553 Hemingway, 1995), and carbonate phases were added (Plummer and Busenberg, 1982;
554 Busenberg et al., 1984; Busenberg and Plummer, 1986; Nordstrom et al., 1990; Robie and

555 Hemingway, 1995). Other data from the LLNL or GWB databases were added even if not
556 identified, and marked as such.

557 *2.1.10.16. Alkaline metals in Column IA*

558 Thermodynamic function of the alkaline $^{I}M^{+}$ free ions are available in CODATA (Cox et
559 al., 1989) and NEA-OECD (Guillaumont et al., 2003) selections. As the interaction between
560 the $^{I}M^{+}$ free ions and ligands are supposed to occur *via* specific ion interaction in SIT, no
561 other complex are taken into account, e.g. $AkHCO_3(aq)$.

562 Concerning solids, data from NEA-OECD (Guillaumont et al., 2003) were complemented
563 by data on oxides (Robie and Hemingway, 1995), sulphur (Harvie et al., 1984; Pankratz et
564 al., 1987; Robie and Hemingway, 1995), carbonates (Wagman et al., 1982; Robie and
565 Hemingway, 1995).

566 *2.2. Modelling*

567 This exercise can be viewed as a benchmark of the PRODATA database itself, having in
568 mind the limitations that are coming from the modeller's choices (Emrén et al., 1999).
569 After the selection of the different water compositions, the obtained results were
570 compared with the different calculations obtained using other available databases, either
571 included in the PhreeqC package or not.

572 2.2.1. PRODATA database file and software version used

573 The PhreeqC version of PRODATA 1.1.0.4 database, extracted on October 26th 2018, was
574 used. It means that later works have not been taken into account in the building of the
575 database (e.g., Jo et al., 2019).

576 The PHREEQC version 3.4.0.12927 (Parkhurst and Appelo, 1999, 2013) was used for the
577 speciation calculation, and Phreeplot 1.0 (Kinniburgh and Cooper, 2004, 2011), which
578 includes a version of PHREEQC 3.4.0.12927, for the calculation of the predominance
579 diagrams. The PHREEQC 3.4.0.12927 was chosen as the stable version at the beginning of
580 the project, i.e. 2015. No difference has been noted in the output results using the more
581 recent version 3.5 in preliminary tests.

582 2.2.2. Software database files for radium

583 There a two database files provided with PhreeqC that allow calculating the speciation of
584 radium, i.e. Thermochimie 9b and LLNL. The database file for the Swiss radioactive waste
585 management program (PSI/NAGRA 12/07) is also containing thermodynamic constants
586 for radium (Thoenen et al., 2014).

587 2.2.3. Software database files for uranium

588 There are four database files provided in the PhreeqC package that allow calculating the
589 uranium speciation, i.e. Thermochimie 9b (Giffaut et al., 2014), LLNL, Wateq4f (Ball and
590 Nordstrom, 1991), and Minteq (EPA, 1998). The PSI/NAGRA 12/07 database file is also
591 containing uranium thermodynamic constants (Thoenen et al., 2014). This latter database
592 file has been built with the specific application field in radioactive waste management and

misses some important data in the field of environmental and mining activities monitoring. Nevertheless, it will give interesting viewpoints on several issues.

After the beginning of this program, NEA-OECD made public a PhreeqC version database file of the selected thermodynamic constants (Martinez et al., 2019). For the reasons explained earlier, this database have not been considered.

2.2.4. Comments on auxiliary and ancillary data

The choice of the auxiliary — directly linked to the uranium or radium chemistry —, or ancillary — linked to species or elements that are linked to uranium and radium — can be important. As an example, the formation of $CaSO_4(aq)$ complexes can be discussed. Within Thermochimie 9b the value comes from Bell and George (1953), when the choice of Sverjensky et al. (1997) is done in PRODATA 1.1.0.4. It is noteworthy that Yeatts and Marshall (1969) proposed even lower $\log_{10}K°$ values based on a wider range of ionic strength.

Knowing the particularly important concentration of total sulphate, or rather SO_4^{2-} activity, implied in an ISR process, this can have an impact on the monitoring of an industrial process. In different cases in the following the consequences of these choices will be shown to have noticeable, but often limited, impact on the theoretical speciation obtained using the different databases.

2.3. Selection of studied water compositions

There is a large body of data on water composition in literature. The main objective of this exercise is to verify the applicability of PRODATA for water that linked to uranium mining

activities, and mostly waters that are under the monitoring of ORANO Mining. In order to have a large body of data, we have chosen to select other water composition, either linked to nuclear energy cycle, or of more general interest.

All solution compositions are given as their PhreeqC input script in the Supplementary Information (SI).

2.3.1. Waters linked to a uranium mine activity

2.3.1.1. Groundwaters in ISR context

In Situ Recovery (ISR) is one of the main mining techniques for Uranium (IAEA, 2001, 2016). Dedicated generally to extract uranium from low-grade deposits in highly permeable geological formations, ISR implies water/rock reactions to enhance the solubility of uranium through oxidative attack and solubilisation in acid or alkaline conditions. We will consider several water compositions taken in an ISR context from ORANO mining sites: from non-acidified waters — TNU_N_18, PZOV_0013_1, PZOV_0001_1, PZOV_0033_1, MOZO_0007_1, MOZO_0009_1, PTZO_0001_1, PZOV_0021_1, PZOV_0022_1, PZOV_0024_1, and ISRW_0001 in Figures S1-1 to S1-11 of the SI — to moderately — TNU_N_39 Figures S1-12 and S1-13 of the SI — and highly acidified waters — TNU_N_37 and ISRW_0098 in Figure S1-14 and Figure S1-15 of the SI. These cases will be complemented by water compositions directly at the input — Entrée Usine in Figure S1-16 of the SI — and the outlet — Sortie Usine in Figure S1-17 of the SI — of a mill. The pH values, sulphate concentrations, and redox conditions are the main chemical parameters for which variations are observed concurrently with aqueous uranium concentrations.

2.3.1.2. Waters sampled in the vicinity of uranium mining sites

Concurrently to waters taken in ISR context, we considered several waters sampled in the vicinity of mining sites: either upstream — i.e. without any mining activity influence — ARLI_3082, RVA1, and Henriette in Figures S2-1 to S2-3 of the SI — or within the mining sites — i.e., under anthropic influence, COMI_79, ES-85, CHD3, V105, BD200, PT4 Rejet in Figures S2-4 to S2-9 of the SI. The pH values, sulphate, and carbonate concentrations are the main chemical parameters for which variations are observed concurrently with aqueous uranium concentrations.

These waters compositions are complemented by the uranium mining pile where the $Ca_nUO_2(CO_3)_3^{(4-2n)-}$ complexes were first evidenced (Bernhard et al., 1996) — results are presented in Figure S2-10 of the SI.

2.3.1.3. Waters sampled downstream former uranium mine

In a recent publication, Stetten et al. (2018) studied the speciation of uranium in a lacustrine sediment (Lac Saint-Clément) impacted by the former uranium mine of Bois Noirs Limouzat in France. The authors proposed the composition of waters from 4 cores at different depths. We selected core C4, which is the more complete dataset, containing U and Fe(II) concentration, which allows calculating speciation and redox conditions. The concentration of dissolved organic carbon are available but will not be used within the framework of this exercise. This example will only be treated using PRODATA 1.1.0.4 database file.

2.3.1.4. Cluff Lake former uranium mine

At the former Cluff Lake uranium mine, von Gunten et al. (2018) studied the uranium content in two meromictic lakes. The authors calculated the theoretical speciation from the water compositions using PhreeqC and the Minteq database — output file were kindly provided by the corresponding author. Results are presented in Figure S4-1 to S4-8 of the SI.

2.3.2. Radioactive waste management

Water compositions in underground research laboratories (URL) for radioactive waste management have been proposed. In France, the water compositions from clayey environments were proposed: the Callovo-Oxfordian was proposed by Gaucher et al. (2009) — results in Figures S5-1 of the SI —, and the water from Tournemire by Beaucaire et al. (2008) — results in Figure S5-2 and S5-3 of the SI. In Belgium, the Boom clay water composition is proposed in de Craen et al. (2004) — result in Figure S5-4 of the SI. In Switzerland, the Mont-Terri tunnel has been thoroughly studied, and water compositions from the clay environment can be found in Courdouan Merz (2008) and Thury and Bossart (1999), and results are presented in Figure S5-5 to S5-7 of the SI. In Sweden, a reference granite water composition for the site of Äspö can be found in Emrén et al. (1999), and the results are shown in Figure S5-8 of the SI. As no uranium concentrations are reported in these water compositions, the calculations were performed at equilibrium with crystalline UO_2 — except for PSI/NAGRA 12/07 database which excludes the crystalline phase — considering no perturbation of the water

677 compositions given the buffering capacity of the host rock, even if this latter hypothesis
678 can eventually be discussed (Emrén et al., 1999).

679 2.3.3. FOREGS

680 These waters are issued from the general dataset generated through the European project
681 FOREGS (Forum of European Geological Surveys), and can be considered in a first
682 approach as non-impacted waters. Details are given in Lartigue et al. (submitted). Results
683 are presented in Figure S6-1 to S6-8 of the SI. The general water compositions can be
684 downloaded at http://weppi.gtk.fi/publ/foregsatlas/ForegsData.php.

685 2.3.4. Other sources

686 The migration of uranium has been monitored in a uranium impacted podzol in the
687 French Landes of Gascony (Crançon, 2001; Crançon and Van der Lee, 2003; Crançon et al.,
688 2010). The composition of the water is mildly acidic and carbonated. Results are
689 presented in Figure S7-1 of the SI.

690 Investigating the uranium contain in groundwaters of Al-Batin Alluvial Fan (southern
691 Iraq), Alkinani et al. (2016) provide the composition of the sample W43, which will be
692 included in the pool of water composition. Results are presented in Figure S7-2 of the SI.

693 Prat et al. (2009) provided the composition of Finnish well waters that are rather
694 concentrated in uranium. The $Ca_nUO_2(CO_3)_3^{(4-2n)-}$ complexes were calculated to be
695 predominant, and were observed in time-resolved luminescence spectroscopy. Results
696 from this exercise are presented in Figure S7-3 to S7-15 of the SI.

2.3.5. Canadian aquitard

Ranville et al. (2007) studied the weak association of natural organic matter (NOM) with uranium in an aquitard highly concentrated in Mg, Ca, sulphate, and carbonate (Hendry and Wassenaar, 2000). The formation of $^{II}M_nUO_2(CO_3)_3^{(4-2n)-}$ complexes has been shown to prevent the formation of U-NOM complexes (Reiller et al., 2012). Nevertheless, the resulting ionic strengths within the majority of these waters were outside the validity of the used activity correction (Davies, 1962). These waters were included in the exercise, and results are presented in Figure S8-1 to S8-8 of the SI.

2.3.6. Oklo

The natural nuclear reactors in Oklo have been the subject of a rich literature. The Okélobondo uraninite body has been the subject of a blind prediction modelling exercise using several water compositions (Duro et al., 2000a; Duro et al., 2000b). Water compositions from these exercises can be retrieved in Gurban et al. (2000) for Bagombé, and Salas and Ayora (2004) for Okélobondo. Results are presented in Figure S9-1 to S9-15 of the SI for Okélobondo and in Figure S9-16 to S9-18 of the SI for Bagombé.

2.3.7. Standard seawater

Seawater represents an important source of uranium (OECD, 2014) of over 4 billion tU, but at a very dilute concentration (3-4 ppb). The speciation of uranium is a major problem for the uranium recovery from seawater, as well as the one from potential competitor, to develop a method of extraction. From recent theoretical speciation exercise, and from synthetic water experimental observations, the speciation of uranium in seawater is

718 expected to be controlled by carbonate species (Maloubier et al., 2015). Millero et al.
719 (2008) proposed a standard composition for seawater — nearly charge balanced —,
720 which will be used in this work. Results are presented in Figure S10-1 of the SI.

721 **3. Results and Discussions**

722 *3.1. General comments on results*

723 The output files from the different calculations as well as the detailed repartitions of
724 species for uranium and radium for all the cases studied are provided as SI. In the case of
725 uranium, estimations of the uncertainty of the speciation results were attempted. The
726 uncertainties of the calculation using Prodata was done using the simplistic
727 approximation of the propagation of errors varying the $\log_{10}\beta°$, and eventual $\varepsilon(M^+, X^-)$ or
728 $\Delta_r H_m^o$, values for the main species. More sophisticated approaches could be applied — see
729 e.g. Ekberg and Ödegaard-Jensen (2011) —, but are currently out of the framework of the
730 project.

731 *3.2. Radium*

732 Radium is only present in the waters analysed in the framework of the monitoring of
733 mining activities from Orano Mining. PRODATA 1.1.0.4, Thermochimie 9b, LLNL, and
734 PSI/NAGRA 12/07 databases include Ra data, and only PRODATA 1.1.0.4, Thermochimie
735 9b, and PSI/NAGRA 12/07 are including $RaSO_4(aq)$, the presence of which is crucial for
736 monitoring data from mining activities — LLNL only includes Ra^{2+} in solution, see SI.

737 From calculations using the PRODATA 1.1.0.4 database file, evolution of radium
738 speciation as a function of calculated $\alpha(SO_4^{2-})$ is shown in Figure 1; comparable results

739 are obtained using Thermochimie 9b and PSI/NAGRA 12/07 databases, and only differ
740 from slightly different choices of auxiliary data and from activity corrections, see SI. The
741 free ion Ra^{2+} is major at low calculated $a(SO_4^{2-})$ values in non-anthropized waters.
742 Conversely, $RaSO_4(aq)$ is major in the strongly anthropized waters, i.e. for water that are
743 strongly impacted by mining activities at $\log_{10}\left(a(SO_4^{2-})\right) > -2.4$.

744 It must be noted that radium total concentrations in natural waters in natural waters and
745 in mining environments are controlled in many cases by coprecipitation with other
746 alkaline earth sulphate phases — i.e., celestite and barite (Curti et al., 2010; Lestini et al.,
747 2019) —, and also adsorption onto clay minerals (Reinoso-Maset and Ly, 2016; Robin et
748 al., 2017), ferric (oxi-)hydroxide (Sajih et al., 2014), and organic matter (Bordelet et al.,
749 2018). Nevertheless, this would not drastically change the general speciation results.

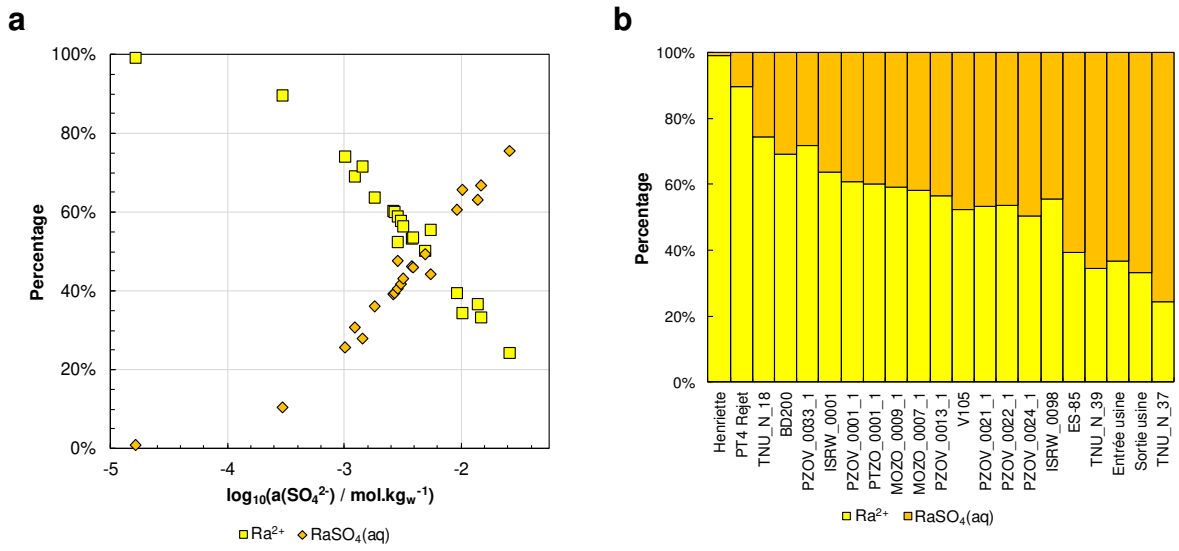

Figure 1. Evolution of the repartition of radium species in selected waters containing sulphate using the PRODATA 1.1.0.4 database and SIT ionic strength correction: (a) as a function of calculated $\log_{10}\left(a\left(SO_4^{2-}\right)\right)$; and (b) identification of waters in the order of calculated $a\left(SO_4^{2-}\right)$.

3.3. Uranium

3.3.1. General results

From a general point of view, it can be seen in the SI that uranium speciation results are mostly the same for PRODATA 1.1.0.4 and Thermochimie 9b databases. This is mainly due to the same body of data (Guillaumont et al., 2003; Dong and Brooks, 2006) and the same activity correction. Some slight differences are occurring at temperature different from 25°C for ${}^{II}M_nUO_2(CO_3)_3^{(4-2n)-}$ complexes, as the enthalpy determinations from Endrizzi and Rao (2014) are included in PRODATA 1.1.0.4. One can also remind that other species than $Ca_nUO_2(CO_3)_3^{(4-2n)-}$ are not considered in Thermochimie 9b. In the following, except explicitly noted, the results can be considered the same for uranium between these two

764 databases, and the results from the calculations using PRODATA 1.1.0.4 will mainly be
765 discussed.

766 *3.3.1.1. Uncertainties*

767 The uncertainties of the speciation results also confirm that PRODATA 1.1.0.4 and
768 Thermochimie 9b are providing comparable results. One of the the largest uncertainty is
769 coming from the formation of $(UO_2)_2CO_3(OH)_3^-$, which is given in Guillaumont et al.
770 (2003) as

771 $2UO_2^{2+} + 4H_2O + CO_2(g) \rightleftarrows (UO_2)_2CO_3(OH)_3^- + 5H^+ \quad \log_{10}\beta° = -19.01 \pm 0.50$

772 and is expressed as follows in PRODATA.

773 $2UO_2^{2+} + 3H_2O + CO_3^{2-} \rightleftarrows (UO_2)_2CO_3(OH)_3^- + 3H^+ \quad \log_{10}\beta° = -0.86 \pm 0.50$

774 This large uncertainty value is responsible of the large error bars on Figure S2-3a and S7-
775 1 of the SI.

776 The other large uncertainty is coming from cumulative uncertainty of the solubility of
777 $UO_2(hyd, am)$ and fourth hydrolysis of U^{4+}.

778 $UO_2(hyd, am) + 4H^+ \rightleftarrows U^{4+} + 2H_2O \quad \log_{10}K° = 1.5 \pm 0.03$

779 $U^{4+} + 4H_2O \rightleftarrows U(OH)_4(aq) + 4H^+ \quad \log_{10}\beta° = -10.01 \pm 1.40$

780 $UO_2(hyd, am) + 2H_2O \rightleftarrows U(OH)_4(aq) \quad \log_{10}K° = -8.51 \pm 1.40$

781 This explains the large uncertainties in Figure S5-5 and S5-6, and to a lesser extend in
782 Figure S4-5.

783 *3.3.1.2. Main differences between database files*

784 In LLNL database file, it seems that the uranium data are taken from the original uranium
785 NEA review (Grenthe et al., 1992). It can be seen for some cases that the $UO_2(OH)_2(aq)$
786 complex can be major in the LLNL cases — e.g. Figures S2-3, S4-6, S4-7, S4-8, S6-1, S7-1,
787 S9-3, S9-4, S9-5, S9-8, and S9-14 of the SI — or at least show some importance — e.g.
788 Figures S1-11, S1-12a, S2-9, S4-1, S4-2, S4-3, S6-6, S6-7, S6-8, S7-14, S9-12, S9-16, S9-17,
789 and S9-18 of the SI.

790 It is noteworthy that the $UO_2H_2PO_4^+$ complex contributes as a minor species in acidic
791 media (Figures S1-14, S1-16, and S1-17 of the SI) in LLNL output data. This is due to a
792 difference in the $\log_{10}\beta°$ value.

793 For the equilibrium

794 $UO_2^{2+} + HPO_4^{2+} + H^+ \rightleftarrows UO_2H_2PO_4^+ \qquad \log_{10}\beta° = 11.54$

795 in LLNL, when for NEA-OECD the equilibria

796 $UO_2^{2+} + H_3PO_4(aq) \rightleftarrows UO_2H_2PO_4^+ + H^+ \quad \log_{10}\beta° = 1.12 \pm 0.06$

797 is expressed as

798 $UO_2^{2+} + HPO_4^{2+} + H^+ \rightleftarrows UO_2H_2PO_4^+ \qquad \log_{10}\beta° = 10.47 \pm 0.07$

799 calculated in PRODATA 1.1.0.4 from Guillaumont et al. (2003) from the selected $\Delta_f G_m^o$.

In Wateq4f and Minteq databases, the data from the more recent review are used (Guillaumont et al., 2003), but the $^{II}M_nUO_2(CO_3)_3^{(4-2n)-}$ complexes are not present. In the light of the common use of Minteq database in the geochemical community, we will principally compare the results from PRODATA 1.1.0.4 database to the Minteq one. A marked difference is the occurrence of $UO_2(HPO_4)_2^{2-}$ complex in Wateq4f (Ball and Nordstrom, 1991) and Minteq (EPA, 1998) results, which is not selected in the NEA-OECD review — after reinterpretation of original data in Grenthe et al. (1992) — and thus not present either in PRODATA 1.1.0.4, Thermochimie 9b, or PSI/NAGRA 12/07. It is noteworthy that the $\log_{10}\beta°(UO_2(HPO_4)_2^{2-})$ values are different in Wateq4f and Minteq — $\log_{10}\beta°$ = 43.44 and 42.99 for Wateq4f and Minteq, respectively, which explains the slight difference in speciation results. This complex is occurring for Wateq4f and Minteq output results (Figures S7-2, S7-3, S7-4, S7-7 of the SI), but can be a major species (Figures S1-14, S2-1, S7-11, S7-12, S7-13, S7-14 of the SI) outcompeting $UO_2(CO_3)_n^{(2-2n)+}$ complexes. This is inducing a major difference in the theoretical speciation results, which has also been emphasized in Wang et al. (2019). Because of the non-selection of this complex in NEA-OECD (Grenthe et al., 1992) (vide supra), the implication of this complex will not be discussed further.

Concerning the $^{II}M_nUO_2(CO_3)_3^{(4-2n)-}$ complexes, Thoenen et al. (2014) proposed slightly different data from PRODATA 1.1.0.4 and Thermochimie 9b, as the value for $\log_{10}\beta°(MgUO_2(CO_3)_3^{2-})$ is chosen from Dong and Brooks (2006), and $\log_{10}\beta°(Ca_2UO_2(CO_3)_3(aq))$ is chosen from Kalmykov and Choppin (2000). The activity coefficient of $Ca_2UO_2(CO_3)_3(aq)$ is fixed to 1 in Thoenen et al. (2014) for this neutral species, even if one can remark that Kalmykov and Choppin (2000) evidenced a marked

ionic strength dependence on $\log_{10}\beta(Ca_2UO_2(CO_3)_3(aq))$. One can remind that this evolution is strongly discussed in Guillaumont et al. (2003), and is at the centre of the non-selection of the thermodynamic data. This latter value is lower than the one proposed by Dong and Brooks (2006), which was extrapolated using Davies (1962) equation.

3.3.1.3. Repartition of the main species

The repartition of the major species obtained after calculation using PRODATA 1.1.0.4 is shown in an Eh-pH plot in Figure 2 — the same repartition is awaited for Thermochimie 9b following the companion study (Lartigue et al., submitted). It can be seen that only nine complexes are controlling the speciation of uranium for the selected waters. The free uranyl, UO_2^{2+}, dominates in low pH and low carbonated non-anthropized waters. The $UO_2(SO_4)(aq)$ complex, dominates in all the anthropized waters where uranium extraction are (or were) occurring. The $UO_2(CO_3)(aq)$ complex, dominated for mildly acidic and carbonated waters, as also calculated in others instances (Neiva et al., 2019). The $U(OH)_4(aq)$ complex, dominates in highly reductive conditions. The $(UO_2)_2CO_3(OH)_3^-$ complex dominates in only one context of a podzol (Crançon, 2001), because of the relatively mildly acidic pH, high uranium and carbonate concentrations. Finally, the $UO_2(CO_3)_2^{2-}$ and $Ca_nUO_2(CO_3)_3^{(4-2n)-}$ complexes — with $n = \{0; 1; 2\}$ — are dominating in a wide region from mildly acidic to mildly basic carbonated waters, with no apparent systematic repartition — this results is slightly more complicated than the predominance Pourbaix diagram provided by Maher et al. (2013), which was considering only one calcium concentration. It can nevertheless be noted already that in the case of reducing waters — like the ones from envisaged underground radioactive waste

management sites (de Craen et al., 2004; Gaucher et al., 2009) — that $CaUO_2(CO_3)_3^{2-}$ or $Ca_2UO_2(CO_3)_3(aq)$ are calculated to be major species — see e.g. Grivé et al. (2015).

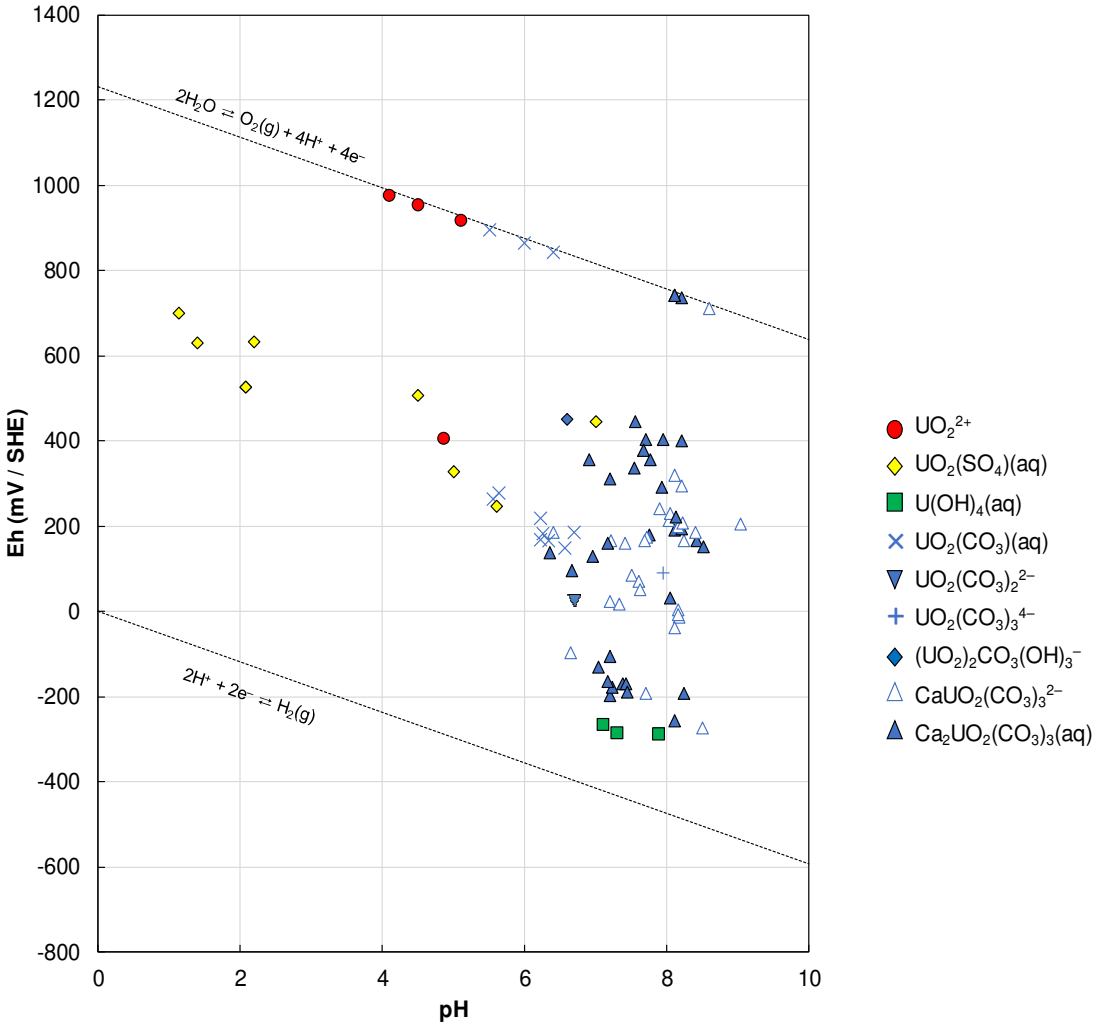

Figure 2. Major uranium species obtained in the speciation calculations of the different waters considered using the PRODATA 1.1.0.4 database and SIT ionic strength correction in the Eh-pH domain.

Figure 3 is showing the repartition of the same major species in a Piper plot. The strongly anthropized waters containing high concentration of sulphate — i.e. more than 80% —, and showing the $UO_2(SO_4)(aq)$ complex as major species, are containing more Ca and Mg

compared to Na^+ and K^+. The waters that are showing $UO_2(CO_3)(aq)$ complex as major species do not seem to have a particular localization in the Piper plot. Concerning the $Ca_nUO_2(CO_3)_3^{(4-2n)-}$ complexes, it can be seen that they seem to be more likely regrouped along the bisectrix Ca(0%)-Mg(50%), and in the lower part of the bisectrix Ca(100%)-Na+K (50%).

The repartition of the major species in a $\log_{10}[U]_{total} - \log_{10}([C(IV)] + [S(VI)])$ diagram (Figure S11-1 of the SI) shows the wide distribution of total uranium concentration. It seems that the higher the S(VI) concentration, the higher the total uranium concentration, but there is no particular trend.

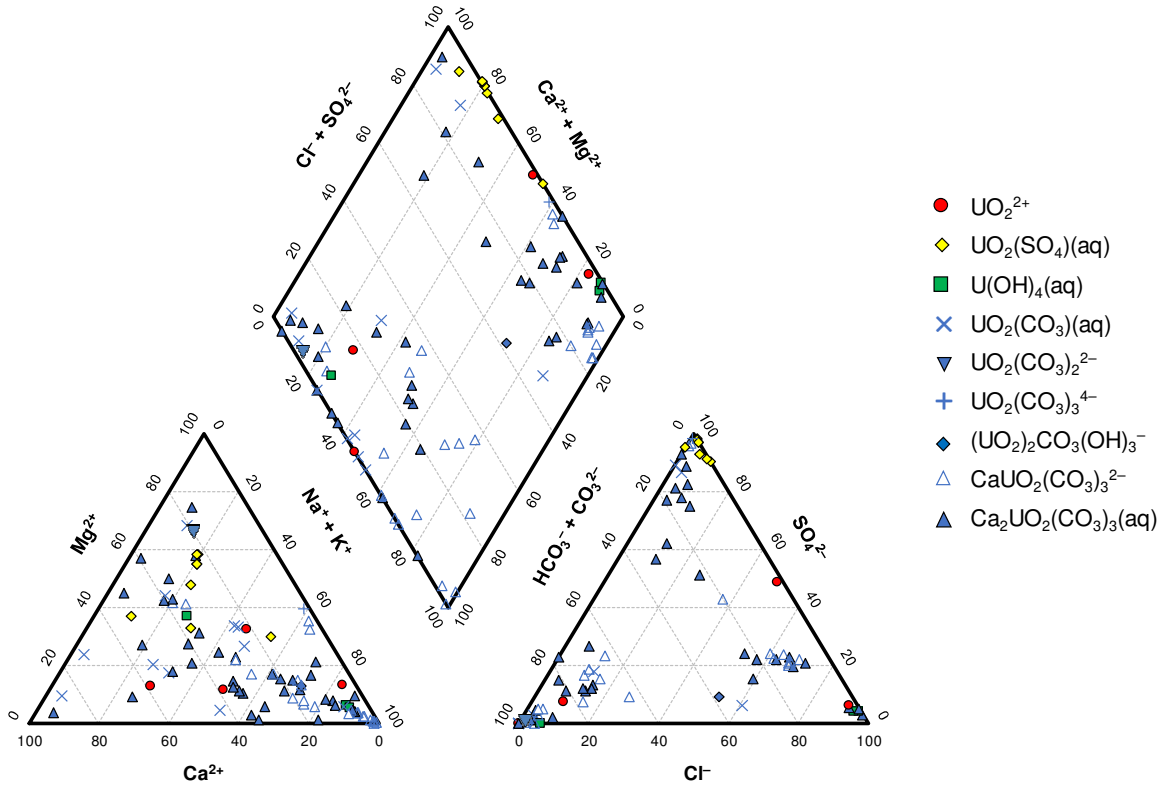

Figure 3. Piper plot for the major species obtained in the speciation calculations of the different waters considered using the PRODATA 1.1.0.4 database and SIT ionic strength correction.

3.3.2. Mining activities monitoring: effect of sulphate

The first interesting domain that can be identified in Figure 2 is due to the dominance of $UO_2(SO_4)(aq)$ complex. These waters are mainly corresponding to anthropized waters implied in the monitoring of mining activities. In the following section, we will focus on these waters emphasizing on the influence of the activity of SO_4^{2-}.

3.3.2.1. Calculation in the framework of PRODATA 1.1.0.4 database

The obtained speciation results are shown as percentages for the mining activity waters in Figure 4 — similar results are obtained using the Thermochimie 9b database, see SI. In Figure 4a only the $UO_2(SO_4)_n^{(2-2n)+}$ complexes are shown as a function of the calculated $\log_{10}\left(a(SO_4^{2-})\right)$. More complete speciation results including more than 5% complexes are shown on Figure 4b with the water origin in increasing order of $a(SO_4^{2-})$. Using SIT, $UO_2(SO)_4(aq)$ is the major complex when $-3 < \log_{10}\left(a(SO_4^{2-})\right) < -1.5$. With increasing $a(SO_4^{2-})$, the percentage of $UO_2(SO_4)_2^{2-}$ becomes increasingly important, and $UO_2(SO_4)_3^{4-}$ is noticeable at the highest $a(SO_4^{2-})$ value. This can have an impact on the efficiency of the ion exchange resins used in an ISR process. The output results are mostly the same for Thermochimie 9b, LLNL, Wateq4f and PSI/NAGRA 12/07 databases with slight differences that are due to different choices of auxiliary data and activity corrections. The Minteq database outputs are showing significant differences, which will be discussed in the next section (*vide infra*).

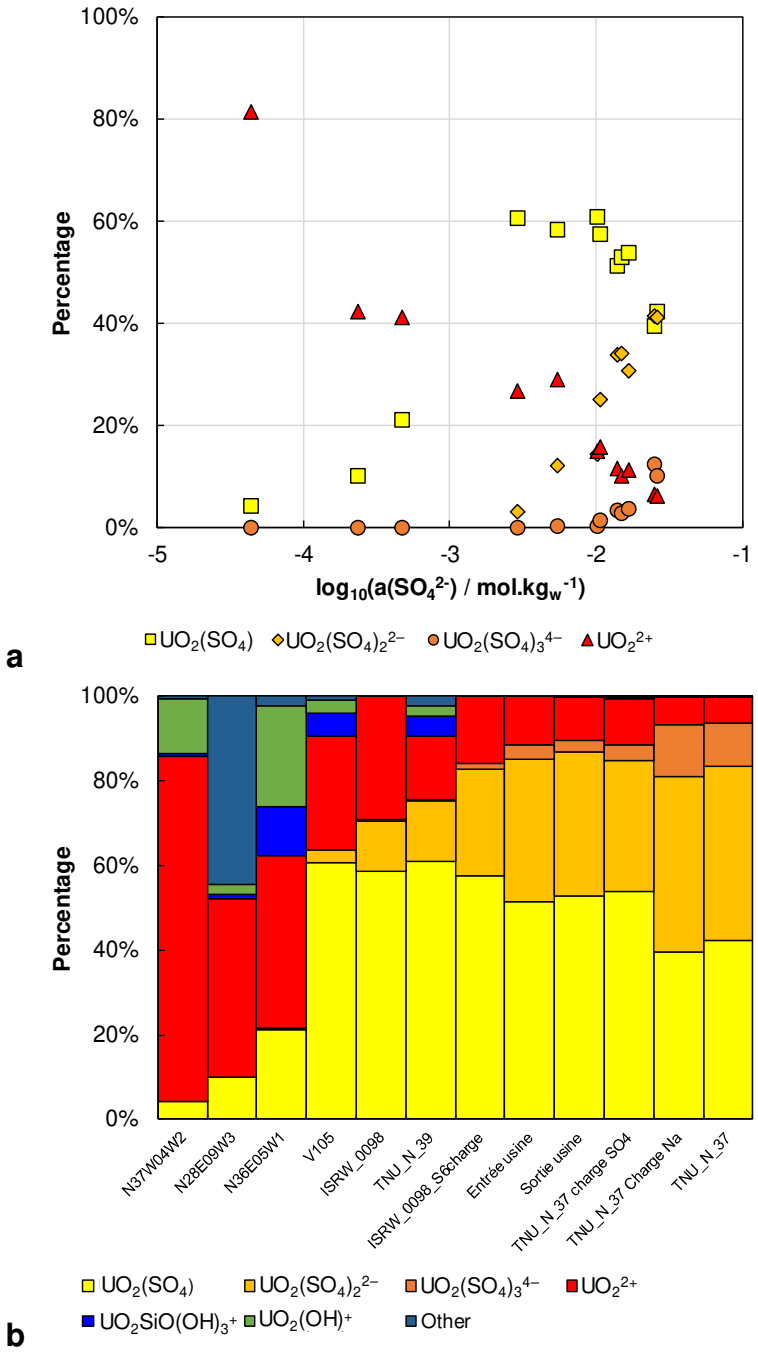

884 **Figure 4. Evolution of the repartition of uranium species in selected sulphated**
885 **waters calculated using the PRODATA 1.1.0.4 database and SIT ionic strength**
886 **correction as a function of (a) calculated $a(SO_4^{2-})$, and (b) the origin of the waters.**

887 *3.3.2.2. Impact of the chosen database*

888 In addition to the earlier comment (cf. § 3.3.1), the particular effect of the choices of the
889 database and activity correction for speciation calculations is shown through the analysis
890 of the differences between the calculation using PRODATA 1.1.0.4 (Figure 4) and the
891 results obtained using the Minteq database (Figure 5). For these water compositions,
892 main differences come from the choice of $\log_{10}\beta°(UO_2(SO_4)(aq))$. In PRODATA 1.1.0.4
893 — and also in Thermochimie 9b and PSI/NAGRA 12/07 — the value from Guillaumont et
894 al. (2003) ($\log_{10}\beta°(UO_2(SO_4)(aq))$ = 3.15 ± 0.02) is chosen, whereas a lower value is
895 chosen in the Minteq database ($\log_{10}\beta°\left(UO_2(SO_4)\right)$ = 2.709). Hence, UO_2^{2+} is major at low
896 $a(SO_4^{2-})$ value, and $UO_2(SO_4)_2^{2-}$ is major at $\log_{10}\left(a(SO_4^{2-})\right) > -2$. It is noteworthy that the
897 $\log_{10}\beta°(UO_2(SO_4)_2^{2-})$ values only differ by 0.04 between the two databases — this
898 difference is less than the uncertainty of $\log_{10}\beta°(UO_2(SO_4)_2^{2-})$ = 4.14 ± 0.07 in
899 Guillaumont et al. (2003) —, and that $\log_{10}\beta°(UO_2(SO_4)_3^{4-})$ is absent from the Minteq
900 database — and also from the LLNL and Wateq4f databases. This can have an impact on
901 the theoretical speciation concerning the monitoring of an ISR process.

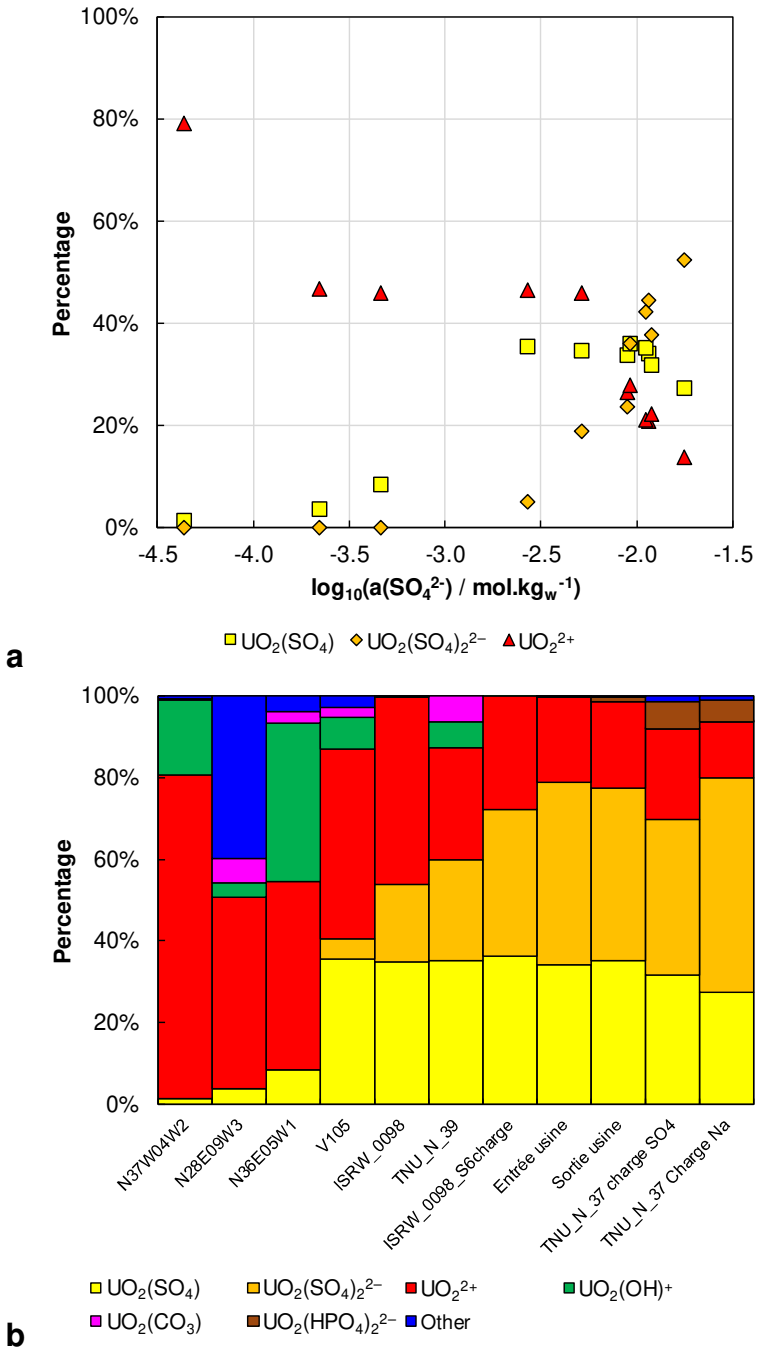

902 **Figure 5. Evolution of the repartition of uranium species in selected sulphated**
903 **waters calculated using the Minteq database as a function of (a) calculated $a(SO_4^{2-})$,**
904 **and (b) the origin of the waters sorted in the order of calculated $a(SO_4^{2-})$.**

3.3.3. Environmental monitoring: effect of Ca^{2+}

The second most striking region in Figure 2 is the occurrence of the $Ca_nUO_2(CO_3)_3^{(4-2n)-}$ complexes. In the following section, we will discuss the repartition of these complexes.

From the plot in Figure 2, it can be seen that the $Ca_nUO_2(CO_3)_3^{(4-2n)-}$ complexes are occurring from oxic mildly acidic and alkaline carbonated waters to slightly reducing waters. No real trend could be evidenced. Kohler et al. (2004) proposed a repartition in the narrow pH range of their study, showing the predominance of the $Ca_2UO_2(CO_3)_3(aq)$ complex, but the wider range of conditions explored here is showing a more intricate repartition.

The representation as a function of $a(CO_3^{2-})$ for the selected waters from the environmental monitoring given in Figure 6a permits only partly understanding the pattern. It seems that the proportion of the $Ca_2UO_2(CO_3)_3(aq)$ complex decreases with $a(CO_3^{2-})$ except for three water compositions, i.e. PZOV_0021_1 (Figure S1-8 of the SI), PZOV_0022_1 (Figure S1-9 of the SI), PZOV_0024_1 (Figure S1-10 of the SI). The proportion of $UO_2(CO_3)_2^{2-}$ in ARLI 3082 — $\log_{10}\left(a(CO_3^{2-})\right)$ = –5.45, Figure S2-1 of the SI — does not fit with the general pattern too. In Figure 6c it can be seen that the $a(Ca^{2+})$ of these waters are the lowest.

However, plotting the obtained speciation of selected waters from environmental monitoring *vs.* calculated $\log_{10}\left(a(Ca^{2+})\right)$ in Figure 6b, allows clearly distinguishing the evolution of $CaUO_2(CO_3)_3^{2-}$ from $Ca_2UO_2(CO_3)_3(aq)$ with a crossing point at

$\log_{10}\left(a(Ca^{2+})\right)$ ca. – 3.2 — the origin of the waters are given in Figure 6c in the order of the calculated $a(Ca^{2+})$.

Extending the representation from Figure 6b to all the waters that are showing significant proportions of the $Ca_nUO_2(CO_3)_3^{(4-2n)-}$ complexes yields to the representation given in Figure S12-1a of the SI, which is showing the same pattern even with a slightly higher dispersion — the origin of the waters is given in Figure S12-1b of the SI in the order of the calculated $a(Ca^{2+})$. It is also noteworthy that a large part of these waters are oversaturated relative to calcite ($CaCO_3$) and dolomite ($CaMg(CO_3)_2$) — see in Figure S12-2 of the SI.

As for the previous case of sulphate complexes, differences in obtained speciation of carbonate complexes is shown in Figure S12-3 of the SI when using the Minteq database. The evolution of $UO_2(CO_3)_n^{(2-2n)+}$ percentage is typically evolving with calculated $a(CO_3^{2-})$ — $^{II}M_nUO_2(CO_3)_3^{(4-2n)-}$ complexes are not implemented in the database.

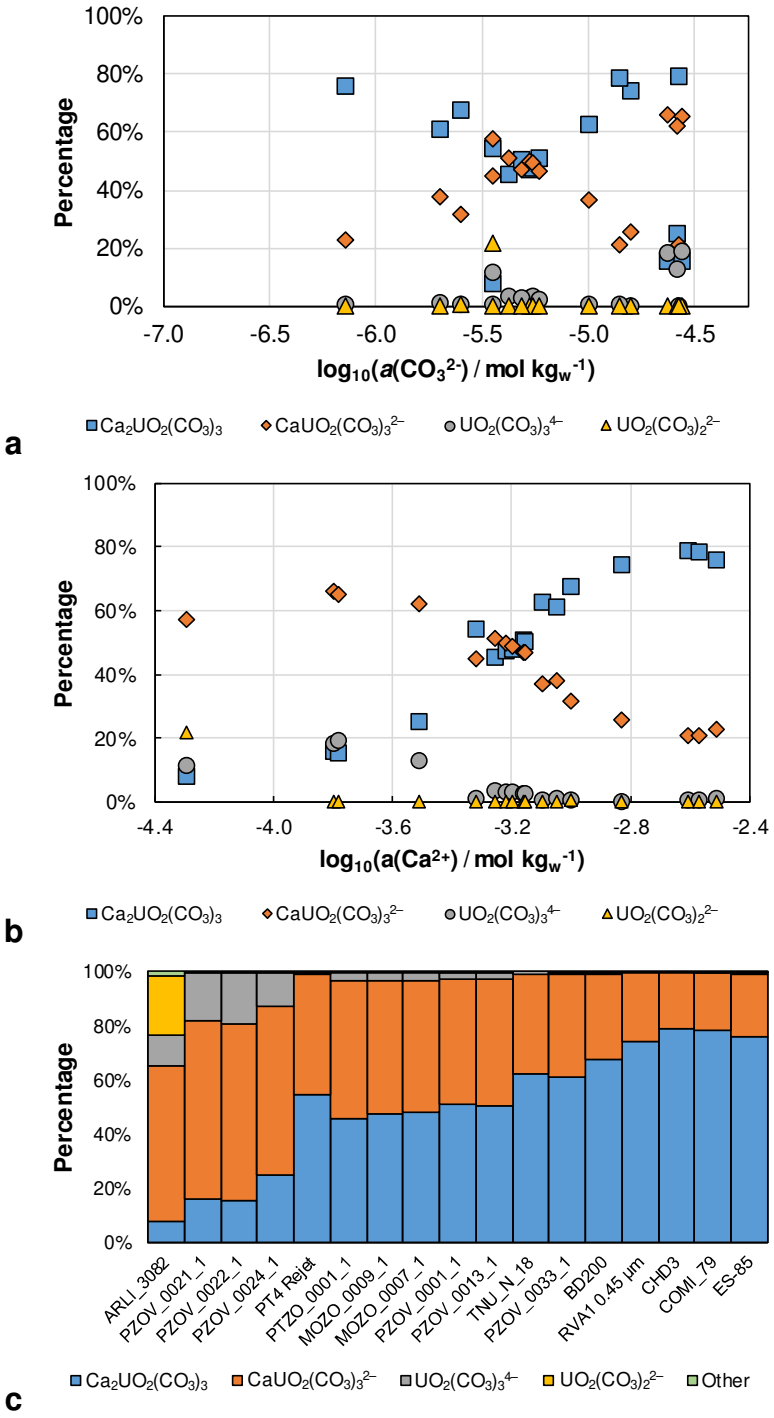

Figure 6. Evolution of repartitions of uranium species in selected carbonated waters linked to the monitoring of mining activities using the PRODATA 1.1.0.4 database and SIT ionic strength correction as a function of calculated (a) $a(\mathrm{CO_3^{2-}})$, (b) $a(\mathrm{Ca^{2+}})$, and (c) origin of the waters in the order of calculated $a(\mathrm{Ca^{2+}})$.

3.3.4. Effect of Eh

Uranium is a redox sensitive element. The oxidation/reduction reactions are very important in the formation of ores (Langmuir, 1978), and are at the center of the radioactive waste management in deep geological formation. Under its +IV redox state, uranium is highly insoluble either as oxide, phosphate, or silicate. In the next section, we will focus on the results from waters representative of nuclear waste management sites — to test the wider applicability of PRODATA 1.1.0.4 —, and some other waters linked to environmental monitoring.

3.3.4.1. Radioactive waste management

Depending on national contexts, the disposal of nuclear wastes is envisaged in deep geological formations, where reducing conditions assure low solubility of actinides, and particularly of uranium. The repartition of the different species obtained in the calculations using PRODATA 1.1.0.4 database are given in Figure 7 as a function of different parameters: (i) the influence of redox potential (Figure 7a), represented *via* the *p*e values;

$$p\mathrm{e} = \frac{F\,\mathrm{E_h}}{RT\ln(10)} \tag{10}$$

(ii) the influence of the calculated $a(\mathrm{Ca}^{2+})$ (Figure 7b); and (iii) the Ca^{2+} and CO_3^{2-} activities *vs. p*e (Figure 7c). From a general point of view, the results obtained with PRODATA are comparable to the one with the dedicated waste management databases, i.e. Thermochimie 9b and PSI/NAGRA 12/07. In the case of PSI/NAGRA 12/07 database

961 the choice of the $MgUO_2(CO_3)_3^{2-}$ complex from Dong and Brooks (2006) and using Davies
962 (1962) equation for activity correction is slightly favouring the complex compared to the
963 PRODATA 1.1.0.4 results. It can be seen that redox potential has an important influence
964 on the uranium speciation, but does not allow fully understanding the general pattern.
965 For instance, the waters that are showing the three lowest *p*e values, are showing different
966 speciation — $U(OH)_4(aq)$ for BWS-A1 (pH = 7.3, pe = –4.82, Figure S5-5 of the SI) and
967 BWS-A2 (pH = 7.1, *p*e = –4.51, Figure S5-6 of the SI), and $CaUO_2(CO_3)_3^{2-}$ for Mol reference
968 water (pH = 8.5, *p*e = –4.78, Figure S5-4 of the SI),. The combination with Figure 7c shows
969 that $\log_{10}\left(a(Ca^{2+})\right)$ and $\log_{10}\left(a(CO_3^{2-})\right)$ have opposite — and mostly mirrored — trends,
970 which allows understanding that even if BWS-A1 — and to a lesser extent BWS-A2 — is
971 showing the mostly same *p*e value as Mol reference water — and higher $\log_{10}\left(a(Ca^{2+})\right)$
972 value —, the more important pH and carbonate contents — or overall the more important
973 $\log_{10}\left(a(CO_3^{2-})\right)$ value — is leading to the stabilisation of U(VI) as $CaUO_2(CO_3)_3^{2-}$ complex
974 for Mol reference water.

975 One can also notice that in the PSI/NAGRA 12/07 database, the $UCO_3(OH)_3^-$ is added as a
976 "maximum feasible value for ternary hydroxide-carbonate complexes of U(IV)…" to
977 account for the influence of carbonate on the actinides(IV) oxides solubility (Thoenen et
978 al., 2014), based on a study of Hummel and Berner (2002). This species is usually minor
979 except for the most reductive potentials — i.e., BWS-A1 (Figure S5-5) and BWS-A2 (Figure
980 S5-6), where it is clearly the major species, and Äspö (Figure S5-8) to a lesser extent.
981 Further works are clearly needed to ascertain the influence of this species on the solubility
982 product of UO_2 phases.

983 Equivalent to Figure 7a, Figure S13-1 of the SI is showing the repartition of species vs. *p*e
984 for the calculation using Minteq database. Uranium(IV) controls the speciation under the
985 form of $U(OH)_5^-$ whatever the conditions, as $^{II}M_nUO_2(CO_3)_3^{(4-2n)-}$ are not implemented
986 in the database. It is noteworthy that $U(OH)_5^-$ is not selected in NEA-OECD selection
987 (Guillaumont et al., 2003).

988 The choice of the database can have here again a strong influence on the calculated
989 equilibrium concentration of uranium under the conditions of an underground storage,
990 or disposal, site of radioactive waste.

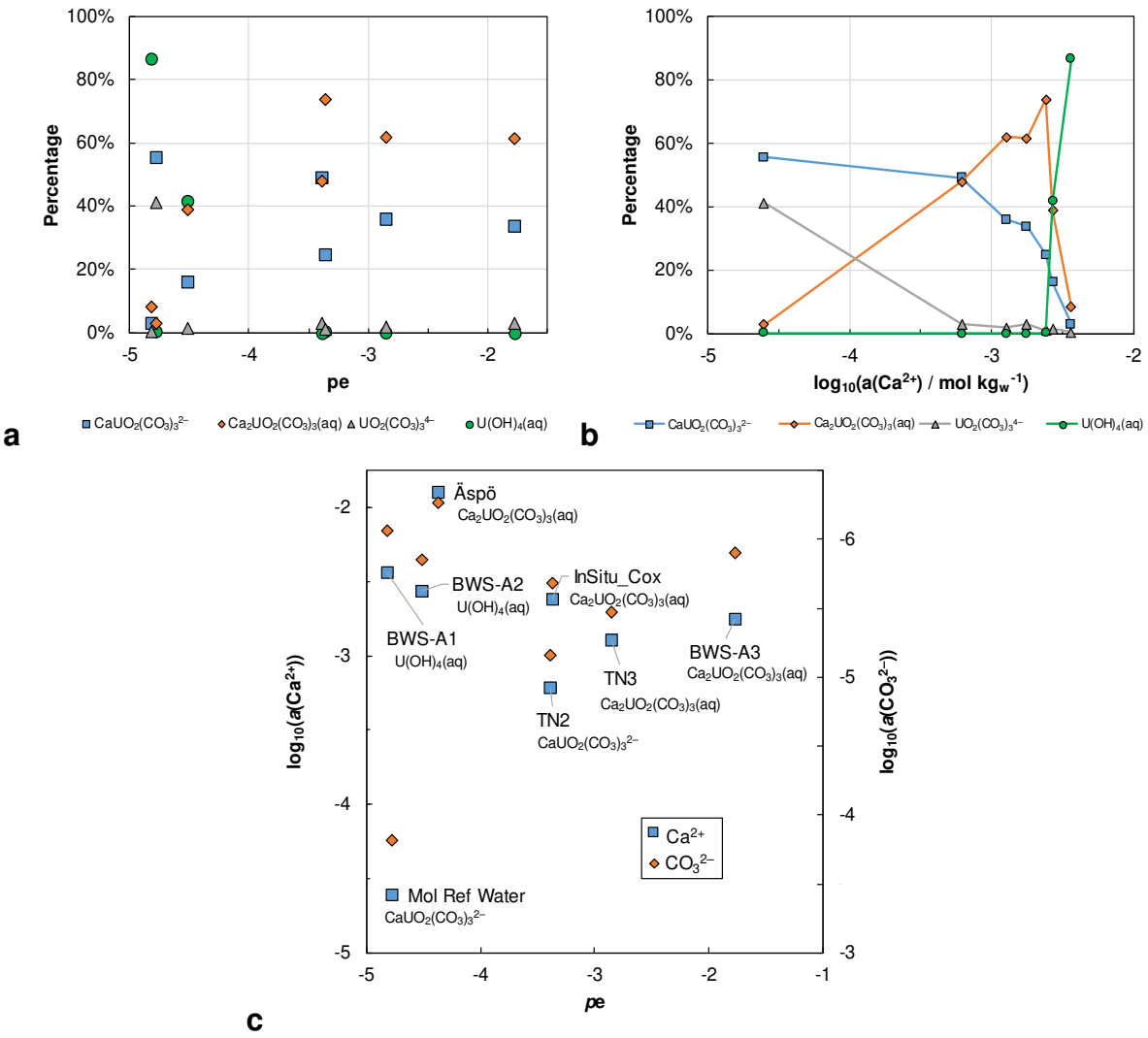

991 **Figure 7. Evolution of the uranium species for the radioactive waste management**
992 **waters using PRODATA 1.1.0.4 database and SIT ionic strength correction as a**
993 **function of *pe* (a), and $\log_{10}\left(a(Ca^{2+})\right)$ (b); and plot of the $\log_{10}\left(a(Ca^{2+})\right)$ and**
994 **$\log_{10}\left(a(CO_3^{2-})\right)$ vs. *pe* (c).**

995 *3.3.4.2. Lac Saint-Clément, Bois Noirs U mine*

996 In their recent publication, Stetten et al. (2018) estimated the speciation of uranium in
997 solution of a lacustrine sediment near the former mine of Bois Noirs Limouzat (France).

The authors calculated the uranium speciation using JCHESS geochemical speciation code, but without specifying the database used — the default chess database is guessed. No speciation result was given. The uranium speciation was driven by the Fe(II) amount in the water and no redox potential was reported. The authors estimated the U(IV) repartition assuming that either ningyoite ($CaU(PO_4)_2{:}\,2H_2O$) or amorphous UO_2 could precipitate. In the default CHESS database, the complexation constant of $U(OH)_4(aq)$ seems based on the Grenthe et al. (1992) analysis, and solubility of $UO_2(am)$ is different from Guillaumont et al. (2003).

For this exercise we performed the calculation using only PRODATA 1.1.0.4 database file. The obtained equilibrium redox potentials, as *p*e values, are those that can be calculated from the Fe^{3+}/Fe^{2+} couple. As in section 3.3.3 (vide ante), the $Ca_nUO_2(CO_3)_3^{(4-2n)-}$ complexes are dominant and are increasing with depth in Figure 8a, but more clearly with $a(Ca^{2+})$ in Figure 8b — Figure 8c is showing the different waters in the order of $a(Ca^{2+})$.

The crossing point in Figure 6b and Figure S12-1a of the SI occurs here at slightly lower $a(Ca^{2+})$ because of the lower *p*e value — and the initial importance of $U(OH)_4(aq)$ —, which can be understood through the combination of $\log_{10}\left(a(Ca^{2+})\right)$ and $\log_{10}\left(a(CO_3^{2-})\right)$ vs. *p*e in Figure S13-2 of the SI, as in Figure 7c (cf. § 3.3.4.1).

The saturation indices in Figure S13-3 of the SI are showing that the water compositions are close to saturation with either ningyoite or $UO_2(am)$ depending on depth. This is in agreement with the dominant U(IV) speciation revealed in the sediment analyses in Stetten et al. (2018).

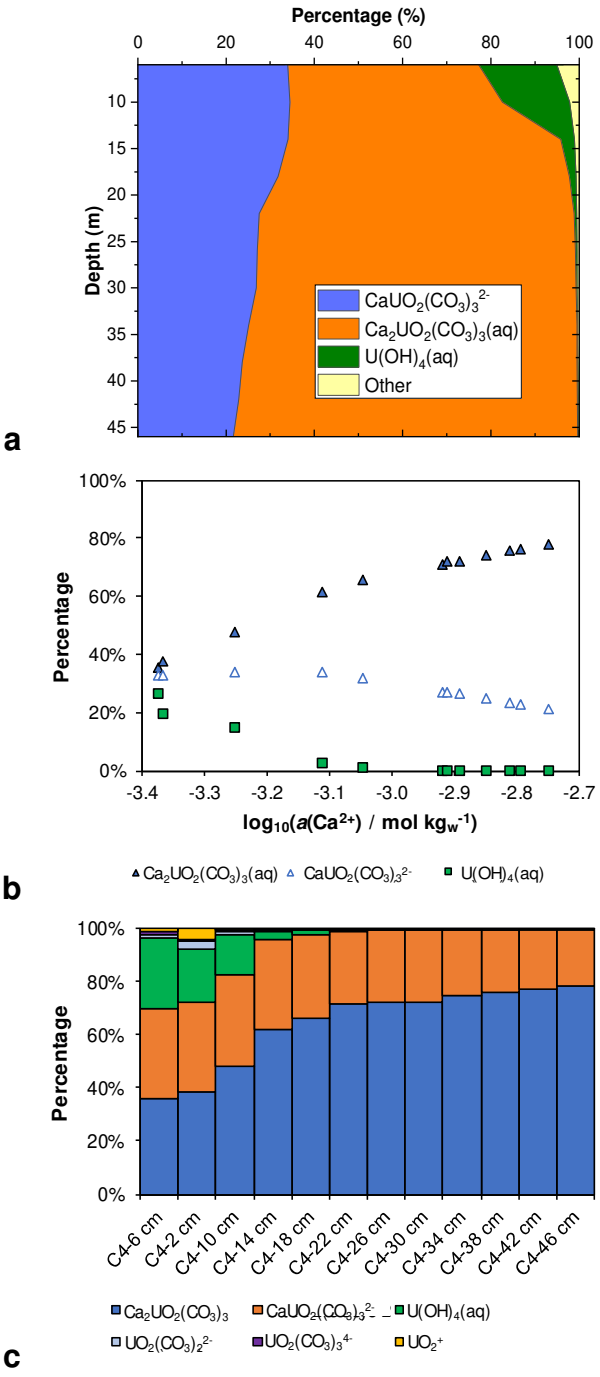

Figure 8. Evolutions of the uranium speciation vs. depth (a), $\log_{10}\left(a(Ca^{2+})\right)$ (b), and origin of the waters using the PRODATA 1.1.0.4 database file and SIT ionic strength correction in the order of calculated $a(Ca^{2+})$ (c) in the water compositions from the core C4 of a lacustrine sediment near the Bois Noirs U mine (in SI of Stetten et al., 2018).

3.3.4.3. Meromictic Lake at the Cluff Lake uranium mine, North Saskatchewan

A recent work from von Gunten et al. (2018) reported speciation calculation in samples from meromictic lakes at the former Cluff Lake uranium mines (Saskatchewan, Canada). The authors performed their calculations using the Minteq database provided with PhreeqC proposing that in the D-pit lake, uranium was controlled by oxic chemistry, under the form of U(VI) from the lake surface down to 10 m depth, and was reduced to U(IV) at depth lower than 13 m. Using the output files form the calculation provided by the authors, the same calculations were performed with all databases. The representations in Figure 9 illustrate the results using PRODATA 1.1.0.4 (Figure 9a) and Minteq (Figure 9b) databases. The results obtained with Minteq database confirm the calculated reduction of uranium. Nevertheless, the results obtained using PRODATA 1.1.0.4 are showing a slightly different pattern. The $Ca_nUO_2(CO_3)_3^{(4-2n)-}$ complexes are calculated to be dominant from the surface down to 13 m; only at 20 m depth do U(IV) is major in the form of the $U(OH)_4$(aq) complex — and $U(OH)_3^+$ complex to a lesser extent.

The evolution of calculated speciation results vs. $a(CO_3^{2-})$ on Figure S13-4 of the SI, shows the influence of U(VI)/U(IV) ratio in these waters. It is also interesting to note that dissolved CH_4(aq) is not implemented in the Minteq database, which implies a higher $a(CO_3^{2-})$ value compared to the calculation with other databases that do contain CH_4(aq). The evolution of the SI for U(IV) containing phases (Figure S13-5 of the SI) is showing that even if the U(VI)/U(IV) limit in solution can be slightly moved down from 10 to 13 m considering Minteq or PRODATA 1.1.0.4, UO_2(am) seems to be the controlling phase lower than 10 m in both cases.

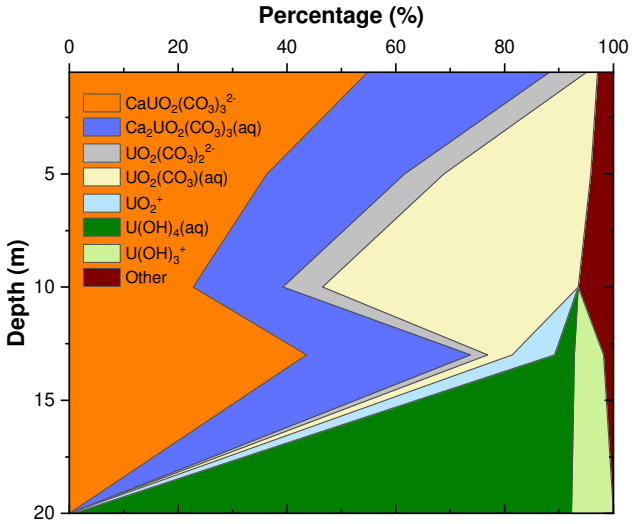

a

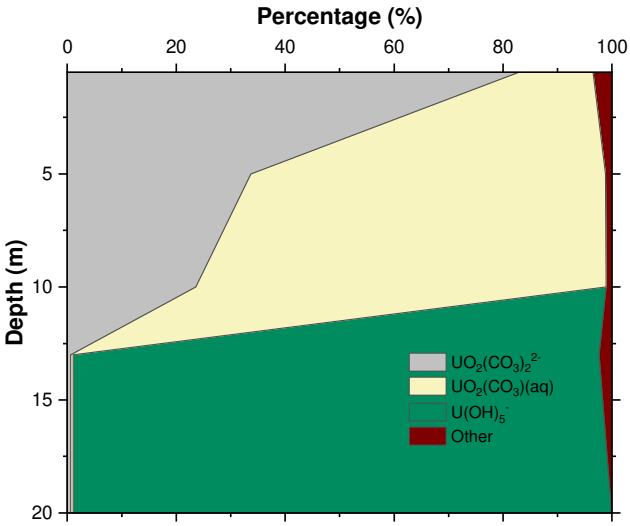

b

Figure 9. Comparison of species repartition for the calculation in the D-pit lake at Cluff Lake uranium mine (von Gunten et al., 2018) using PRODATA 1.1.0.4 database file and SIT ionic strength correction (a) and Minteq (b) database file.

3.3.4.4. Aquitard, South Saskatchewan

The last example is the uranium speciation in a highly sulphated aquitard in south Saskatchewan (Canada) — see Hendry and Wassenaar (2000) —, where the eventual

association with natural organic matter was tested by Ranville et al. (2007). Theoretical calculation already confirmed that uranium was not associated significantly to natural organic matter (Reiller et al., 2012) under these conditions, but the ionic strength was not correctly accounted as high concentrations of Ca, Mg and sulphate were reported in these waters (Hendry and Wassenaar, 2000). Concentrations of carbonate and pH values also imply that the $^{II}M_nUO_2(CO_3)_3^{(4-2n)-}$ complexes — with $^{II}M^{2+}$ being either Mg^{2+} or Ca^{2+}, and n = $\{0; 1; 2\}$ — control the uranium speciation instead of natural organic matter (Reiller et al., 2012). Using the water composition from Hendry and Wassenaar (2000) and the uranium concentrations from Ranville et al. (2007), the repartition of uranium species as a function of depth is shown in Figure 10a for PRODATA 1.1.0.4 and Figure 10b for Minteq databases. Here again the particular importance of the $^{II}M_nUO_2(CO_3)_3^{(4-2n)-}$ complexes is clearly shown. A total reduction of U(VI), mainly as $UO_2(CO_3)_3^{4-}$, to U(IV) as $U(OH)_5^-$, is calculated at depth higher between 6 and 9 m using Minteq database (Figure 10b), whereas uranium is calculated under U(VI) form at whatever depth (Figure 10a) using PRODATA 1.1.0.4. The speciation of the $^{II}M_nUO_2(CO_3)_3^{(4-2n)-}$ complexes can be explained in two ways: (i) there is a variation in the ratio Mg/Ca vs. depth that can help understanding the decrease in $Ca_2UO_2(CO_3)_3(aq)$ proportion and increase of $CaUO_2(CO_3)_3^{2-}$ and $MgUO_2(CO_3)_3^{2-}$ (Figure 11a); (ii) there is a high variation of calculated ionic strength from 1.41 mol kg_w^{-1} at 2.3 m, down to 0.07 mol kg_w^{-1} at 30.4 m (Figure 11b).

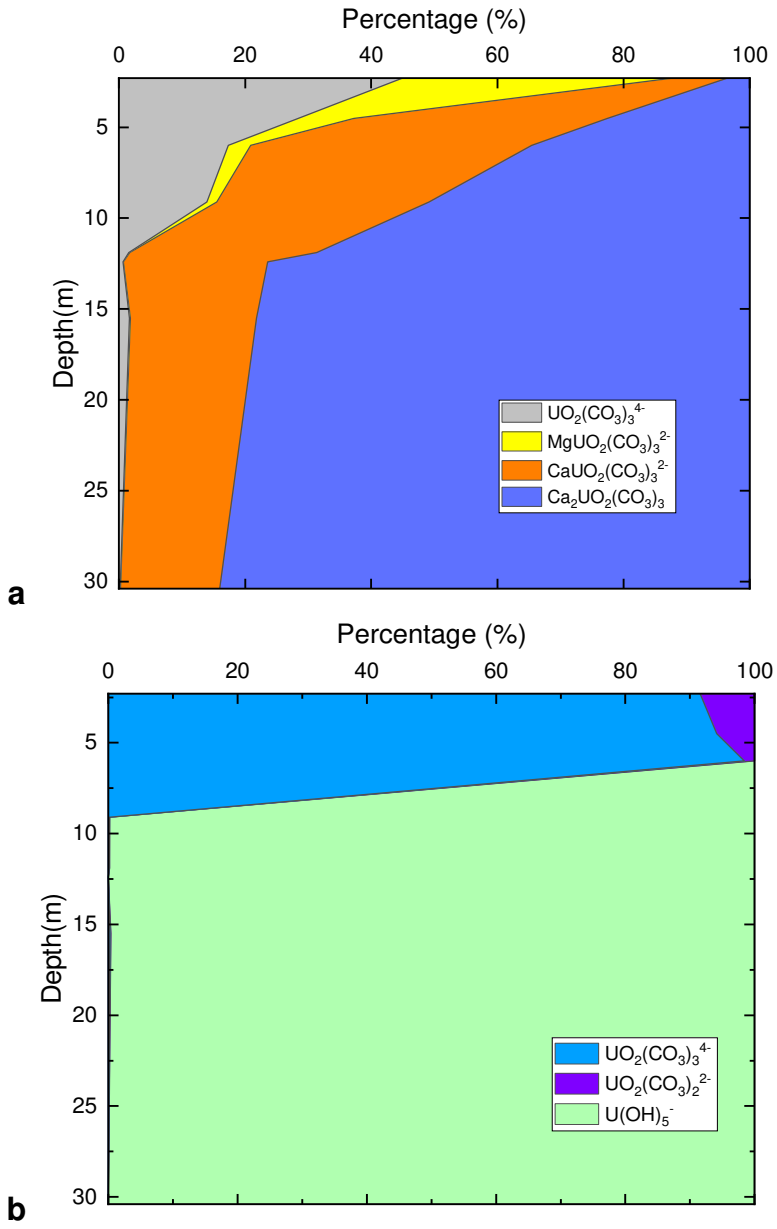

Figure 10. Comparisons of uranium species repartitions as a function of depth using (a) PRODATA 1.1.0.4 database file and SIT ionic strength correction, and (b) Minteq database file, in the case of a Canadian Aquitard (Hendry and Wassenaar, 2000; Ranville et al., 2007).

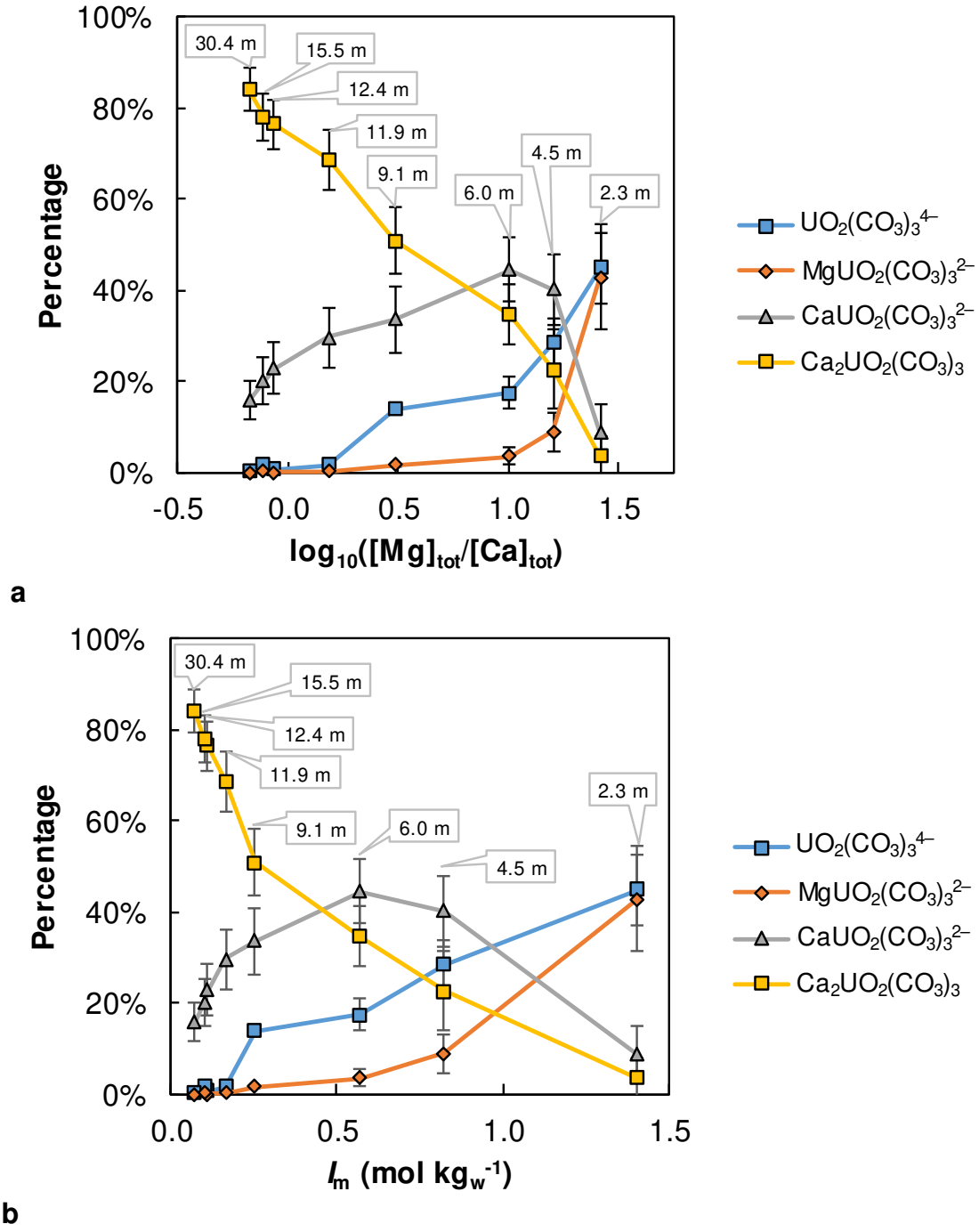

Figure 11. Uranium species repartition vs. Mg/Ca ratio (a) and calculated ionic strength (b) using PRODATA 1.1.0.4 database file and SIT ionic strength correction, in the case of a Canadian Aquitard (Hendry and Wassenaar, 2000; Ranville et al., 2007). Lines are guides to the eye.

3.3.5. Effect of activity correction

3.3.5.1. Impact of the choice of $log_{10}\beta°(MgUO_2(CO_3)_3^{2-})$ and activity correction

As seen in this exercise (vide supra), the impact of the choice for the complexation constant of $MgUO_2(CO_3)_3^{2-}$ can be somewhat important. As an illustration, the evolution of $\log_{10}\beta(MgUO_2(CO_3)_3^{2-})$ as a function of ionic strength (Figure S14-1 of the SI) implies a relatively lower importance of the complex when using Dong and Brooks (2008) and the specific ion interaction parameter with Na^+, i.e. $\varepsilon(MgUO_2(CO_3)_3^{2-}, Na^+)$, than using the value determined by Dong and Brooks (2006) and the Davies (1962) equation at I_m < 0.4 mol kg_w^{-1}; but the situation is inversed at I_m > 0.4 mol kg_w^{-1}. This explain partly both the evolution of $MgUO_2(CO_3)_3^{2-}$ proportion in radioactive waste management waters using the PSI/NAGRA 12/07 database (c.f. § 3.3.4.1), and in the Canadian aquitard (c.f. § 3.3.4.4). It can also be evidenced that the ionic strength dependence of $\log_{10}\beta(MgUO_2(CO_3)_3^{2-})$ has not received sufficient attention up to now.

One can also remind that using the SIT defined in PhreeqC is implying that if the ε value of a complex relative to a counter ion is not given, then its value is considered nil. The calculation is not strictly equivalent to the calculation using the Davies (1962) equation — see Grenthe et al. (1997) for detailed analysis.

The implication of the alkali metals, which was suggested by the review from Guillaumont et al. (2003), is also suspected from molecular dynamics study (Li et al., 2017). A particular effort seems to be needed to tackle this particular point.

3.3.5.2. Particular case of seawater

In addition to the preceding examples, one can have a closer look to the results in Figure S10-1 of the SI. The already discussed differences induced by the account of the $^{II}M_nUO_2(CO_3)_3^{(4-2n)-}$ complexes in the different database files is apparent here again. One can have a closer look at the differences between e.g., PRODATA 1.1.0.4 —formatted for SIT formalisms — and Thermochimie 9b results, obtained using SIT, and the theoretical speciation proposed by Maloubier et al. (2015), where the choice of the activity correction is not clearly stated, and is guessed to be a simplified Debye-Hückel relation. Notwithstanding the fact that $MgUO_2(CO_3)_3^{2-}$ complex was not considered, the predominance of $Ca_2UO_2(CO_3)_3(aq)$ (ca. 70%) over $CaUO_2(CO_3)_3^{2-}$ (ca. 30%), and nearly inexistence of $UO_2(CO_3)_3^{4-}$, is not observed in our results using SIT, where $Ca_2UO_2(CO_3)_3(aq)$ and $CaUO_2(CO_3)_3^{2-}$ are mostly equal and $UO_2(CO_3)_3^{4-}$ is much more important — 19% if $MgUO_2(CO_3)_3^{2-}$ is not considered (data not shown). One has to remind that using eq. 9, as no $\varepsilon(CaUO_2(CO_3)_3^{2-}, Na^+)$ is given in the database, then it is considered nil. Nevertheless, the results from Maloubier et al. (2015) are directly comparable with the proportions obtained using the database file dedicated to the Davies (1962) equation calculation — Prodata Davies in Figure S10-1 of the SI —, which enlightens the need of an accurate determination of both the thermodynamic constants and SIT parameters. As no direct determination of these specific ion interaction parameters are existing for $Ca_nUO_2(CO_3)_3^{(4-2n)-}$ complexes, it is currently not possible to propose a definitive answer on which case is closer to the reality. Further determinations and assessments of the constants and ε values are required.

This also clearly shows the importance of the choice of the activity correction model to provide reliable speciation calculations for monitoring activities.

3.3.6. Rationale on uranium results

To cover the widest possible space of conditions relevant to mining and environmental monitoring activities, some water compositions are plotted in a $\log_{10}\left(a(SO_4^{2-})\right)$ vs. pH predominance plots at fixed total uranium, $-\log_{10}\left(P_{CO_2}\right)$, i.e. pCO_2, $-\log_{10}([Ca]_{tot})$, i.e. pCa, and $-\log_{10}([Mg]_{tot})$, i.e. pMg, constructed using PhreePlot (Figure 12). The choice of the values of pCO_2, pCa, and pMg are based on the analysis of the frequency of these parameters in waters that are showing $Ca_nUO_2(CO_3)_3^{(4-2n)-}$ as major complex (Figure S15-1 of the SI). In these plots, the $a(SO_4^{2-})$ value is fixed adding Na_2SO_4 to the solution. As some waters are oversaturated respective to calcite and dolomite, the precipitation of these phases was not requested during calculation in agreement with the saturation indices (Figure S12-2 of the SI).

The waters that are showing predominantly the free ion UO_2^{2+} or $(UO_2)_2CO_3(OH)_3^-$ at low total Ca and Mg, as major species are correctly represented. Concerning highly anthropized waters, as seen in Figure 3, the cations in these waters are more controlled by Ca^{2+}, Mg^{2+}, and H^+, than by Na^+ and K^+. Hence, the transition between $UO_2(SO_4)(aq)$ and $UO_2(SO_4)_2^{2-}$ is slightly overestimated, but the solutions are correctly represented in every situation at the exception of DJX-pit 50 m at the higher calculated pCO_2. The water from the podzol (Crançon, 2001) is well represented in the two higher pCO_2 cases; the formation of $(UO_2)_2CO_3(OH)_3^-$ is impeded at the higher total Ca value.

Concerning the $^{II}M_nUO_2(CO_3)_3^{(4-2n)-}$ complexes, $CaUO_2(CO_3)_3^{2-}$ can only be represented in the second case (Figure 12b), with the exception of the Mol Reference Water, which is also well represented in the highest total Ca value. The $Ca_2UO_2(CO_3)_3(aq)$ complex is well represented under the conditions of the highest total Ca value. The $MgUO_2(CO_3)_3^{2-}$ complex only occurs at high calculated $a(SO_4^{2-})$ — at thus high ionic strength, see Figure 12c. This could be considered as a bias from the choice that has been made on the original data from Dong and Brooks (2008).

The predominance domains of the $^{II}M_nUO_2(CO_3)_3^{(4-2n)-}$ complexes can be modified when accounting for the oversaturation for calcite and dolomite. Figure S16-1 of the SI is clearly showing a narrowing of the $Ca_nUO_2(CO_3)_3^{(4-2n)-}$ domains — the one of $MgUO_2(CO_3)_3^{2-}$ complex is totally suppressed in the case of dolomite precipitation — calculation not shown.

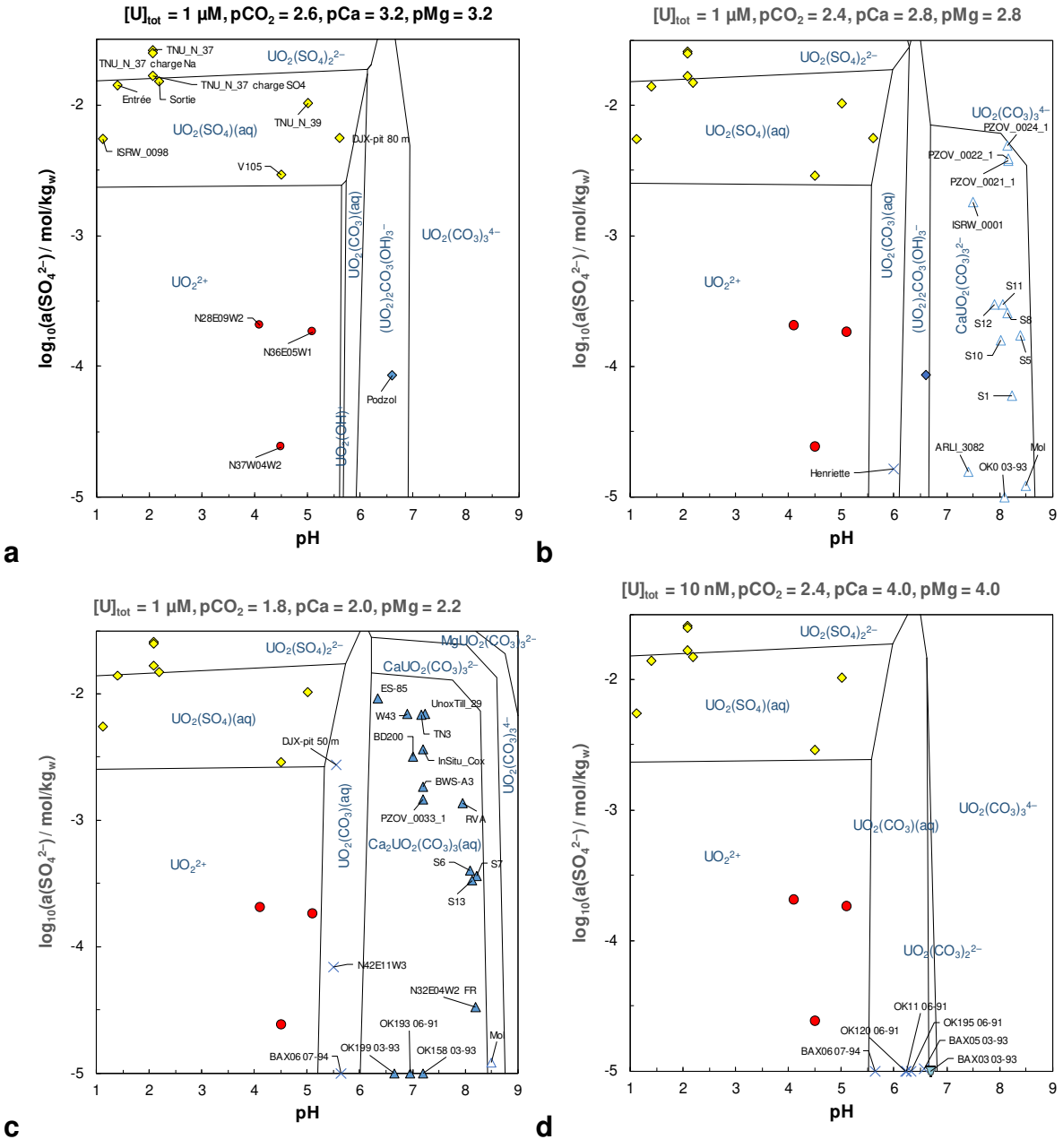

1155 **Figure 12. Predominance plot of the uranium species in the $\log_{10}\left(a\left(SO_4^{2-}\right)\right)$ vs. pH**

1156 **at fixed P_{CO_2} and total Ca and Mg: $[U]_{tot}$ = 1µmol kg_{w}^{-1} using PRODATA 1.1.0.4**

1157 **database file and SIT ionic strength correction. No precipitation of calcite or**

1158 **dolomite is requested during calculation.**

1159 The representation is complemented by Figure 13 at fixed pH values and varying *p*e.
1160 Under low redox conditions, the plot of waters composition relevant of radioactive waste
1161 management are plotted in a $\log_{10}\left(a(Ca^{2+})\right)$ vs. *p*e predominance plot at fixed uranium
1162 concentration constructed using Phreeplot. The $a(Ca^{2+})$ are fixed adding $CaCl_2$. As shown
1163 previously (Figure 7c and Figure S13-2 of the SI), at pH values ca. 7, pCO_2 = 2.2, high
1164 $a(Ca^{2+})$, and low *p*e values, the waters from Mont-Terri that are showing the
1165 predominance of $U(OH)_4(aq)$, and the waters where $Ca_2UO_2(CO_3)_3(aq)$ predominates,
1166 are correctly represented. The water composition from Äspö, which is showing the
1167 highest $a(Ca^{2+})$ value and one of the four lowest E_h value, is also well represented. The
1168 water from the Mol site, which is showing a predominance of $CaUO_2(CO_3)_3^{2-}$, due to its
1169 relatively low $a(Ca^{2+})$ value and relatively high pCO_2 value, is correctly represented at pH
1170 = 8.5 and pCO_2 = 2.6 — the water from Tournemire TN2, which has a pH =7.7 is
1171 necessarily not represented correctly and is not shown.

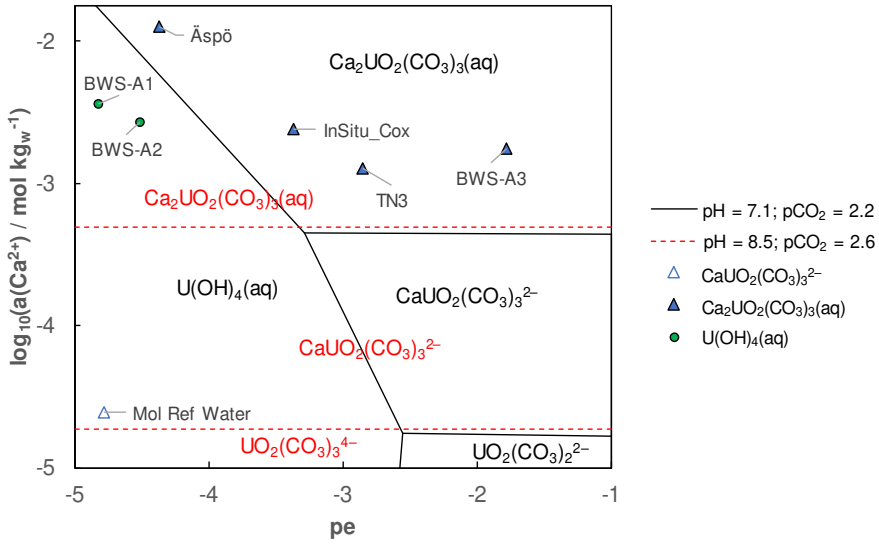

1172 **Figure 13. Predominance plots of the uranium species in the $\log_{10}\left(a(Ca^{2+})\right)$ vs. pe,**
1173 **at fixed pH — pH 7.1 plain line, and pH 8.5 dotted line — and P_{CO_2} and major species**
1174 **obtained in the calculation of selected waters for radioactive waste management**
1175 **using PRODATA 1.1.0.4 database file and SIT ionic strength correction: $[U]_{tot}$ = 1**
1176 **nmol kg_w^{-1}. No precipitation of calcite is requested during calculation.**

1177 ## 4. Conclusions and Perspectives

1178 The use of the PhreeqC database output file from PRODATA 1.1.0.4 database has been
1179 shown to provide valuable information for the speciation of both radium and uranium in
1180 all the aspects of the monitoring of mining activities: from exploration to remediation. It
1181 has also been shown that PRODATA 1.1.0.4 can be applied largely outside of its
1182 development domain, from groundwaters — including aquifer and aquitard —, to stream
1183 waters, and finally to seawaters.

1184 The radium speciation is mainly controlled either by Ra^{2+} or $RaSO_4(aq)$ depending on the
1185 activity of dissolved sulphate, generated particularly by an ISR operation.

The $UO_2(SO_4)_n^{(2-2n)+}$ complexes have been shown to control the speciation in ISR-impacted waters; the use of the $^{II}M_nUO_2(CO_3)_3^{(4-2n)-}$ complexes has been shown to be of particular importance in mildly acidic or alkaline carbonated waters. The thermodynamic constants of these latter complexes are still under discussion as well as their evolution with ionic strength. It is of particular importance that these data will be determined with correct level of confidence as one can remind that these complexes are susceptible to control uranium speciation in seawater (Maloubier et al., 2015; Endrizzi et al., 2016; Beccia et al., 2017).

As the PRODATA database was though as a solution of the use of different database files to estimate a speciation or transport of uranium and radium in the particular contexts of mining and environmental monitoring. This necessarily induces the account for: (i) the major elements contained in the water of the particular site (e.g., Na, K, Ca, Mg, S, C, P…); (ii) the other elements that can be in direct competition with uranium or radium, or directly impact the chemistry of the site (e.g., Fe, Mn, V…); and (iii) the potential secondary contaminants eventually released (e.g., As, Pb, Zn, Cu, Ni…) as part of the ore treatment.

Out of these elements the particular examples of As, Zn, Cu, and Ni are particularly interesting. Significant differences exist between all the different databases for As(III) hydrolysis, As(V)-F(-I), As(V)-U(VI), and As(V)-Ca(II) species. Only Zn^{2+}, Cu^{+}, and Cu^{2+} are implemented in the Thermochimie 9b database file. The $Ni(CO_3)_n^{(2-2n)+}$ complexes are either not present in LLNL, or thermodynamic constants are very different in Minteq and Wateq4f database files compared to the others. It would then be likely to provide a similar exercise with a particular focus on the potential secondary contaminants

encountered in mining or environmental activities monitoring, as proposed otherwise (Katsoyiannis et al., 2007; Neiva et al., 2019).

The PRODATA database is now a tool to perform speciation calculations with different speciation codes using the same body of thermodynamic data for the different elements that are relevant for the monitoring of exploration, exploitation, and finally remediation and environmental monitoring for the mining activities. It will evolve in the future as a function of new determination of constants in the literature, and new (or revised) data selection, e.g., as those currently under review in the TDB project of NEA-OECD. The next step is the use into reactive transport modelling, which requires the implementation of adsorption reactions for U and Ra — e.g. Waite et al. (1994), Murphy et al. (1999), Reinoso-Maset and Ly (2016), Robin et al. (2017), Sajih et al. (2014) —, and also for the other different elements and aqueous species — e.g. Dzombak and Morel (1990), Siroux et al. (2017), Siroux et al. (2018), Wissocq et al. (2018) — that can be in competition, based on the same constraint of traceability.

Declaration of conflict of interest

Pascal E. Reiller is part of the Executive Group of the Thermochemical Data Project from the NEA-OECD as CEA representative. This work is by no mean a support of, or supported by, the Thermodynamic DataBase project of the NEA-OECD.

Acknowledgement

This work was done in the framework of the ORANO-CEA NOPRA program. An anonymous reviewer is warmly welcomed for his suggestions. Dr. Konstantin von Gunten

is acknowledged for kindly providing PhreeqC output. Drs. Tres Thoenen and Wolfgang Hummel are acknowledged for providing the PSI/NAGRA 12/07 Thermochemical database file. PRODATA database is available on demand at prodata@cea.fr.

5. References

Alkinani, M., Kanoua, W., Merkel, B., 2016. Uranium in groundwater of the Al-Batin Alluvial Fan aquifer, south Iraq. Environ. Earth Sci. 75, 869.

Altmaier, M., Metz, V., Neck, V., Müller, R., Fanghänel, T., 2003. Solid-liquid equilibria of $Mg(OH)_2(cr)$ and $Mg_2(OH)_3Cl{\cdot}4H_2O(cr)$ in the system Mg-Na-H-OH-O-Cl-H_2O at 25°C. Geochim. Cosmochim. Acta 67, 3595-3601.

Alwan, A.K., Williams, P.A., 1980. Aqueous chemistry of uranium minerals. Part 2. Minerals of the liebigite group. Mineral. Mag. 43, 665-667.

Ball, J.W., Nordstrom, D.K., 1991. User's Manual for WATEQ4F, with Revised Thermodynamic Data Base and Text Cases for Calculating Speciation of Major, Trace, and Redox Elements in Natural Waters. US Geological Survey, Menlo Park, CA, USA, p. 195. http://pubs.er.usgs.gov/publication/ofr91183

Bard, A.J., Parsons, R., Jordan, J. (Eds.), 1985. Standard Potentials in Aqueous Solution. IUPAC, Marcel Dekker, New York.

Beaucaire, C., Michelot, J.L., Savoye, S., Cabrera, J., 2008. Groundwater characterisation and modelling of water-rock interaction in an argillaceous formation (Tournemire, France). Appl. Geochem. 23, 2182-2197.

Beccia, M.R., Matara-Aho, M., Reeves, B., Rogues, J., Solari, P.L., Monfort, M., Moulin, C., Den Auwer, C., 2017. New insight into the ternary complexes of uranyl carbonate in seawater. J. Environ. Radioactiv. 178-179, 343-348.

Bell, R.P., George, J.H.B., 1953. The incomplete dissociation of some thallous and calcium salts at different temperatures. Trans. Faraday Soc. 49, 619-627.

Beneš, P., Obdržálek, M., Čejchanová, M., 1982. The physicochemical forms of traces of radium in aqueous-solutions containing chlorides, sulfates and carbonates. Radiochem. Radioanal. Lett. 50, 227-241.

Bernhard, G., Geipel, G., Brendler, V., Nitsche, H., 1996. Speciation of uranium in seepage waters of a mine tailing pile studied by time-resolved laser-induced fluorescence spectroscopy (TRLFS). Radiochim. Acta 74, 87-91.

Bernhard, G., Geipel, G., Reich, T., Brendler, V., Amayri, S., Nitsche, H., 2001. Uranyl(VI) carbonate complex formation: validation of the $Ca_2UO_2(CO_3)_3$(aq.) species. Radiochim. Acta 89, 511-518.

Blanc, P., Piantone, P., Lassin, A., Burnol, A., 2006. Thermochimie : Sélection de Constantes Thermodynamiques pour les Éléments Majeurs, le Plomb et le Cadmium. ANDRA, Chatenay-Lamabry, France, p. 157.
http://www.mkg.se/uploads/Arende_SSM2011_2426/SSM20112426_049_Ytterligare_Svar_till_SSM_pa_begaran_angaende_fortydligande_information_om_loslighetsberakningar_bilaga_3.pdf

Bordelet, G., Beaucaire, C., Phrommavanh, V., Descostes, M., 2018. Chemical reactivity of natural peat towards U and Ra. Chemosphere 202, 651-660.

Brown, P., Curti, E., Grambow, B., Ekberg, C., 2005. Chemical Thermodynamics 8. Chemical Thermodynamics of Zirconium. North Holland Elsevier Science Publishers B. V., Amsterdam, The Netherlands. http://www.oecd-nea.org/dbtdb/pubs/vol8-zirconium.pdf

Brown, P.L., Ekberg, C., 2016. Hydrolysis of Metal Ions. Wiley-VCH Verlag GmbH & Co., Weinheim, Germany. http://doi.org/10.1002/9783527656189

Busenberg, E., Plummer, L.N., 1986. The solubility of $BaCO_3$(cr) (witherite) in CO_2-H_2O solutions between 0 and 90 °C, evaluation of the association constants of $BaHCO_3^+$(aq) and $BaCO_3$(aq) between 5 and 80 °C, and a preliminary evaluation of the thermodynamic properties of Ba^{2+}(aq). Geochim. Cosmochim. Acta 50, 2225-2233.

Busenberg, E., Plummer, L.N., Parker, V.B., 1984. The solubility of strontianite ($SrCO_3$) in CO_2-H_2O solutions between 2 and 91 °C, the association constants of $SrHCO_3^+$(aq) and $SrCO_3^0$(aq) between 5 and 80 °C, and an evaluation of the thermodynamic properties of Sr^{2+}(aq) and $SrCO_3$(cr) at 25 °C and 1 atm total pressure. Geochim. Cosmochim. Acta 48, 2021-2035.

Castet, S., Dandurand, J.L., Schott, J., Gout, R., 1993. Boehmite solubility and aqueous aluminum speciation in hydrothermal solutions (90-350°C): Experimental study and modeling. Geochim. Cosmochim. Acta 57, 4869-4884.

Chandratillake, M.R., Newton, G.W.A., Robinson, V.J., 1988. Project Chemval: Comparison of Thermodynamic Databases Used in Geochemical Modelling. Department of the Environment, UK, p. 76.

Chase, M.W. (Ed.), 1998. NIST-JANAF Thermochemical Tables - Fourth Edition. American Chemical Society.

Chen, J.P., Yiacoumi, S., 2002. Modeling of depleted uranium transport in subsurface systems. Water Air Soil Poll. 140, 173-201.

Chivot, J., 2004. Thermodynamique des Produits de Corrosion - Fonctions Thermodynamiques, Diagrammes de Solubilité, Diagrammes E-pH des Systèmes Fe-H_2O, Fe-CO_2-H_2O, Fe-S-H_2O, Cr-H_2O et Ni-H_2O en Fonction de la Température. ANDRA, Chatenay-Malabry, France.

Claret, F., Marty, N., Tournassat, C., 2018. Modeling the long-term stability of multi-barrier systems for nuclear waste disposal in geological clay formations. in: Xiao, Y., Whitaker, F., Xu, T., Steefel, C. (Eds.). Reactive Transport Modeling. John Wiley & Sons Ltd., Oxford, UK, pp. 395-451.

Courdouan Merz, A., 2008. Nature and reactivity of dissolved organic matter in clay formations evaluated for the storage of radioactive waste. ETH Zürich, Zürich, Switzerland, p. 114. http://dx.doi.org/10.3929/ethz-a-005680592

Cox, J.D., Wagman, D.D., Medvedev, V.A., 1989. CODATA Key Values for Thermodynamics. Hemisphere Publishing Corp., New York, USA.

1309 Crançon, P., 2001. Migration de l'Uranium dans un Podzol. Le Rôle des Colloïdes dans la
1310 Zone non Saturée et la Nappe : Application aux Landes de Gascogne. Université de
1311 Grenoble 1, Saint-Martin-d'Hères, Grenoble, France, p. 284.

1312 Crançon, P., Pili, E., Charlet, L., 2010. Uranium facilitated transport by water-dispersible
1313 colloids in field and soil columns. Sci. Total Environ. 408, 2118-2128.

1314 Crançon, P., Van der Lee, J., 2003. Speciation and mobility of uranium(VI) in humic-
1315 containing soils. Radiochim. Acta 91, 673-679.

1316 Cretaz, F., Szenknect, S., Clavier, N., Vitorge, P., Mesbah, A., Descostes, M., Poinssot, C.,
1317 Dacheux, N., 2013. Solubility properties of synthetic and natural meta-torbernite. J. Nucl.
1318 Mater. 442, 195-207.

1319 Curti, E., Fujiwara, K., Iijima, K., Tits, J., Cuesta, C., Kitamura, A., Glaus, M.A., Muller, W.,
1320 2010. Radium uptake during barite recrystallization at 23 ± 2 °C as a function of solution
1321 composition: an experimental ^{133}Ba and ^{226}Ra tracer study. Geochim. Cosmochim. Acta
1322 74, 3553-3570.

1323 Curtis, G.P., Davis, J.A., Naftz, D.L., 2006. Simulation of reactive transport of uranium(VI)
1324 in groundwater with variable chemical conditions. Water Resour. Res. 42, W04404.

1325 Davies, C.W., 1962. Ion Association. Butterworths, London, UK.

de Craen, M., Wang, L., Van Geet, M., Moors, H., 2004. Geochemistry of Boom Clay Pore Water at the Mol site. SCK•CEN, Mol, Belgium, p. 181. http://jongeren.sckcen.be/~/media/Files/Science/disposal_radioactive_waste/Geochemistry_of_Boom_Clay_pore_Status_2004.pdf

Dong, W., Brooks, S.C., 2006. Determination of the formation constants of ternary complexes of uranyl and carbonate with alkaline earth metals (Mg^{2+}, Ca^{2+}, Sr^{2+}, and Ba^{2+}) using anion exchange method. Environ. Sci. Technol. 40, 4689-4695.

Dong, W., Brooks, S.C., 2008. Formation of aqueous $MgUO_2(CO_3)_3^{2-}$ complex and uranium anion exchange mechanism onto an exchange resin. Environ. Sci. Technol. 42, 1979-1983.

Drozdzak, J., Leermakers, M., Gao, Y., Elskens, M., Phrommavanh, V., Descostes, M., 2016. Uranium aqueous speciation in the vicinity of the former uranium mining sites using the diffusive gradients in thin films and ultrafiltration techniques. Anal. Chim. Acta 913, 94-103.

Duro, L., Arcos, D., Bruno, J., 2000a. Blind predictive modelling exercise in Oklo 2nd stage: Uranium in Okélobondo. in: Louvat, D., Michaud, V., von Maravic, H. (Eds.). Oklo Working Groups. Proceedings of the Second EC-CEA Workshop on Oklo-Phase II, Helsinki, 16 to 18 June 1998. European Economic Communities, Luxembourg, pp. 399-409. http://publications.europa.eu/en/publication-detail/-/publication/b8ef3f7d-c345-4597-b779-cf7c00edb895

Duro, L., Arcos, D., Bruno, J., Jordana, S., Grivé, M., Pon, J., Castelier, E., Beaucaire, C., Fauré, M.H., Peña, J., Gimeno, M.J., del Nero, M., Ayora, C., Salas, J., Ledoux, E., Madé , B., 2000b. Blind prediction modelling (BPM) exercise in Oklo. in: Louvat, D., Michaud, V., von Maravic, H. (Eds.). Oklo Working Groups. Proceedings of the Third and Final Joint EC-CEA Workshop on OKLO-Phase II Held in Cadarache, France on 20 and 21 May 1999. European Economic Communities, Luxembourg, pp. 285-305. http://publications.europa.eu/en/publication-detail/-/publication/59044e00-da36-46d2-979a-3ccfd569b20d

Dyrssen, D., Kremling, K., 1990. Increasing hydrogen sulfide concentration and trace metal behavior in the anoxic Baltic waters. Mar. Chem. 30, 193-204.

Dzombak, D.A., Morel, M.M., 1990. Surface Complexation Modelling: Hydrous Ferric Oxide. John Wiley & Sons, New York, NY, USA.

Ekberg, C., Ödegaard-Jensen, A., 2011. Uncertainties in chemical modelling of solubility, speciation and sorption. Accredit. Qual. Assur. 16, 207-214.

Emrén, A.T., Arthur, R., Glynn, P.D., McMurry, J., 1999. The modeler's influence on calculated solubilities for performance assessments at the Äspö Hard-Rock Laboratory. Mater. Res. Soc. Symp. Proc. 556, 559-566.

Endrizzi, F., Leggett, C.J., Rao, L., 2016. Scientific basis for efficient extraction of uranium from seawater. I: understanding the chemical speciation of uranium under seawater conditions. Ind. Eng. Chem. Res. 55, 4249-4256.

Endrizzi, F., Rao, L., 2014. Chemical speciation of uranium(VI) in marine environments: complexation of calcium and magnesium ions with [$(UO_2)(CO_3)_3^{4-}$] and the effect on the extraction of uranium from seawater. Chem.-Eur. J. 20, 14499-14506.

EPA, 1998. MINTEQA2/PRODEFA2, A Geochemical Assessment Model for Environmental Systems: User Manual Supplement for Version 4.0. U.S. Environmental Protection Agency, Athens, GA, USA, p. 81. http://www.epa.gov/sites/production/files/documents/SUPPLE1.PDF

Fabrichnaya, O.B., Saxena, S.K., Richet, P., Westrum, E.F., 2004. Thermodynamic Data, Models, and Phase Diagrams in Multicomponent Oxide Systems. An Assessment for Materials and Planetary Scientists Based on Calorimetric, Volumetric and Phase Equilibrium Data. Sringer-Verlag, Berlin, Germany. http://doi.org/10.1007/978-3-662-10504-7

Felmy, A.R., Dixon, D.A., Rustad, J.R., Mason, M.J., Onishi, L.M., 1998. The hydrolysis and carbonate complexation of strontium and calcium in aqueous solution. Use of molecular modeling calculations in the development of aqueous thermodynamic models. J. Chem. Thermodynamics 30, 1103-1120.

Gailhanou, H., Blanc, P., Rogez, J., Mikaelian, G., Kawaji, H., Olives, J., Amouric, M., Denoyel, R., Bourrelly, S., Montouillout, V., Vieillard, P., Fialips, C.I., Michau, N., Gaucher, E.C., 2012. Thermodynamic properties of illite, smectite and beidellite by calorimetric methods: enthalpies of formation, heat capacities, entropies and Gibbs free energies of formation. Geochim. Cosmochim. Acta 89, 279-301.

Gailhanou, H., Vieillard, P., Blanc, P., Lassin, A., Denoyel, R., Bloch, E., De Weireld, G., Gaboreau, S., Fialips, C.I., Made, B., Giffaut, E., 2017. Methodology for determining the thermodynamic properties of smectite hydration. Appl. Geochem. 82, 146-163.

Gamsjäger, H., Bugajski, J., Gajda, T., Lemire, R.J., Preis, W., 2005. Chemical Thermodynamics 6. Chemical Thermodynamics of Nickel. North Holland Elsevier Science Publishers B. V., Amsterdam, The Netherlands. http://www.oecd-nea.org/dbtdb/pubs/vol6-nickel.pdf

Gaucher, E.C., Tournassat, C., Pearson, F.J., Blanc, P., Crouzet, C., Lerouge, C., Altmann, S., 2009. A robust model for pore-water chemistry of clayrock. Geochim. Cosmochim. Acta 73, 6470-6487.

Giffaut, E., Grivé, M., Blanc, P., Vieillard, P., Colàs, E., Gailhanou, H., Gaboreau, S., Marty, N., Madé, B., Duro, L., 2014. Andra thermodynamic database for performance assessment: ThermoChimie. Appl. Geochem. 49, 225-236.

Grenthe, I., Fuger, L., Konings, R.G.M., Lemire, R.J., Muller, A.B., Nguyen-Trung, C., Wanner, H., 1992. Chemical Thermodynamics 1. Chemical Thermodynamics of Uranium. North Holland Elsevier Science Publishers B. V., Amsterdam, The Netherlands. http://www.oecd-nea.org/dbtdb/pubs/uranium.pdf

Grenthe, I., Plyasunov, A.V., Spahiu, K., 1997. Chapter IX. Estimations of medium effects on thermodynamic data. in: Grenthe, I., Puigdomènech, I. (Eds.). Modelling in Aquatic Chemistry. OECD, Paris, pp. 325-426.

Grenthe, I., Puigdomènech, I., 1997. Modelling in Aquatic Chemistry. Nuclear Energy Agency, OECD, Paris. http://www.oecd-nea.org/dbtdb/pubs/modelling-aquatic-chem.html

Grivé, M., Duro, L., Colàs, E., Giffaut, E., 2015. Thermodynamic data selection applied to radionuclides and chemotoxic elements: an overview of the ThermoChimie-TDB. Appl. Geochem. 55, 85-94.

Guillaumont, R., Fanghänel, T., Fuger, J., Grenthe, I., Neck, V., Palmer, D.A., Rand, M., 2003. Chemical Thermodynamics 5. Update on the Chemical Thermodynamics of Uranium, Neptunium, Plutonium, Americium and Technetium. North Holland Elsevier Science Publishers B. V., Amsterdam, The Netherlands. http://www.oecd-nea.org/dbtdb/pubs/vol5-update-combo.pdf; http://www.oecd-nea.org/dbtdb/pubs/Errata_Update.pdf

Gurban, I., Laaksoharju, M., Ledoux, E., Madé, B., Salignac, A.L., 2000. Indication of uranium transport around the reactor zone at Bangombé (OKLO). in: Louvat, D., Michaud, V., von Maravic, H. (Eds.). OKLO Working Group - Proceedings of the Second EC-CEA workshop on OKLO – Phase II, Helsinki, 16 to 18 June 1998 (EUR 19116 EN). European Commission – Directorate-General for Research, Brussels, Belgium, pp. 273-299.

Harvie, C.E., Møller, N., Weare, J.H., 1984. The prediction of mineral solubilities in natural waters: The Na-K-Mg-Ca-H-Cl-SO_4-OH-HCO_3-CO_3-CO_2-H_2O system to high ionic strengths at 25°C. Geochim. Cosmochim. Acta 48, 723-751.

1428 Helgeson, H.C., Delany, J.M., Nesbitt, H.W., Bird, D.K., 1978. Summary and critique of the
1429 thermodynamic properties of rock-forming minerals. American Journal of Science, Yale
1430 University, New Haven, CN, USA.
1431 http://www.dewcommunity.org/uploads/4/1/7/6/41765907/helgeson_et_al_1978.pdf

1432 Helgeson, H.C., Kirkham, D.H., 1974. Theoretical prediction of thermodynamic behavior
1433 of aqueous electrolytes at high pressures and temperatures: II. Debye-Hückel
1434 parameters for activity coefficients and relative partial molal properties. Am. J. Sci. 274,
1435 1199-1261.

1436 Hendry, M.J., Wassenaar, L.I., 2000. Controls on the distribution of major ions in pore
1437 waters of a thick surficial aquitard. Water Resour. Res. 36, 503-513.

1438 Hummel, W., Anderegg, G., Rao, L.F., Puigdomènech, I., Tochiyama, O., 2005. Chemical
1439 Thermodynamics 9. Chemical Thermodynamics of Compounds and Complexes of U, Np,
1440 Pu, Am, Tc, Se, Ni and Zr with Selected Organic Ligands. North Holland Elsevier Science
1441 Publishers B. V., Amsterdam, The Netherlands. http://www.oecd-
1442 nea.org/dbtdb/pubs/vol9-organic-ligands.pdf

1443 Hummel, W., Berner, U., 2002. Application of the Nagra/PSI TDB 01/01: Solubility of Th,
1444 U, Np and Pu. NAGRA, Wettingen, Switzerland, p. 39.

1445 Hummel, W., Berner, U., Curti, E., Pearson, F.J., Thoenen, T., 2002. Nagra/PSI Chemical
1446 Thermodynamic Data Base 01/01. NAGRA, Wettingen, Switzerland, p. 564.
1447 http://www.nagra.ch/data/documents/database/dokumente/$default/Default%20Fol
1448 der/Publikationen/NTBs%202001-2010/e_ntb02-16.pdf

1449 Hummel, W., Filella, M., Rowland, D., 2019. Where to find equilibrium constants? Sci.
1450 Total Environ. 692, 49-59.

1451 Husson, A., Leermakers, M., Descostes, M., Lagneau, V., 2019. Environmental
1452 geochemistry and bioaccumulation/bioavailability of uranium in post-mining context –
1453 Bois-Noirs Limouzat mine. Chemosphere 236, 124341.

1454 IAEA, 2001. Manual of Acid In Situ Leach Uranium Mining Technology. IAEA, Vienna,
1455 Austria. http://www-pub.iaea.org/MTCD/publications/PDF/te_1239_prn.pdf

1456 IAEA, 2016. In Situ Leach Uranium Mining: An Overview of Operations. IAEA, Vienna,
1457 Austria. http://www-pub.iaea.org/MTCD/Publications/PDF/P1741_web.pdf

1458 Jo, Y., Kirishima, A., Kimuro, S., Kim, H.-K., Yun, J.-I., 2019. Formation of $CaUO_2(CO_3)_3^{2-}$
1459 and $Ca_2UO_2(CO_3)_3(aq)$ Complexes at Variable Temperatures (10 – 70 °C). Dalton Trans.
1460 48, 6942-6950.

1461 Johnson, R.H., Tutu, H., 2016. Predictive reactive transport modeling at a proposed
1462 uranium in situ recovery site with a general data collection guide. Mine Water Environ.
1463 35, 369-380.

1464 Jones, M.J., Butchins, L.J., Charnock, J.M., Pattrick, R.A.D., Small, J.S., Vaughan, D.J., Wincott,
1465 P.L., Livens, F.R., 2011. Reactions of radium and barium with the surfaces of carbonate
1466 minerals. Appl. Geochem. 26, 1231-1238.

1467 Kalmykov, S.N., Choppin, G.R., 2000. Mixed $Ca^{2+}/UO_2^{2+}/CO_3^{2-}$ complex formation at
1468 different ionic strengths. Radiochim. Acta 88, 603-606.

Katsoyiannis, I.A., Hug, S.J., Ammann, A., Zikoudi, A., Hatziliontos, C., 2007. Arsenic speciation and uranium concentrations in drinking water supply wells in Northern Greece: correlations with redox indicative parameters and implications for groundwater treatment. Sci. Total Environ. 383, 128-140.

Kielland, J., 1937. Individual activity coefficients of ions in aqueous solutions. J. Am. Chem. Soc. 59, 1675-1678.

Kinniburgh, D.G., Cooper, D.M., 2004. Predominance and mineral stability diagrams revisited. Environ. Sci. Technol. 38, 3641-3648.

Kinniburgh, D.G., Cooper, D.M., 2011. Creating Graphical Output with PHREEQC. http://www.phreeplot.org

Kohler, M., Curtis, G.P., Meece, D.E., Davis, J.A., 2004. Methods for estimating adsorbed uranium(VI) and distribution coefficients of contaminated sediments. Environ. Sci. Technol. 38, 240-247.

Lagneau, V., Regnault, O., Descostes, M., 2019. Industrial deployment of reactive transport simulation: an application to uranium in situ recovery. Rev. Mineral. Geochem. 85, 499-528.

Langmuir, D., 1978. Uranium solution-mineral equilibria at low temperatures with applications to sedimentary ore deposits. Geochim. Cosmochim. Acta 42, 547-569.

Langmuir, D., Riese, A.C., 1985. The thermodynamic properties of radium. Geochim. Cosmochim. Acta 49, 1593-1601.

1489 Lartigue, J.E., Charrasse, B., Reile, B., Descostes, M., submitted. Aqueous inorganic
1490 uranium speciation in European stream waters from the FOREGS dataset using
1491 geochemical modelling and determination of U bioavailability baseline. Chemosphere
1492 this volume.

1493 Lee, J.-Y., Vespa, M., Gaona, X., Dardenne, K., Rothe, J., Rabung, T., Altmaier, M., Yun, J.-I.,
1494 2017. Formation, stability and structural characterization of ternary $MgUO_2(CO_3)_3^{2-}$ and
1495 $Mg_2UO_2(CO_3)_3(aq)$ complexes. Radiochim. Acta 105, 171-185.

1496 Lee, J.-Y., Yun, J.-I., 2013. Formation of ternary $CaUO_2(CO_3)_3^{2-}$ and $Ca_2UO_2(CO_3)_3(aq)$
1497 complexes under neutral to weakly alkaline conditions. Dalton Trans. 42, 9862-9869.

1498 Lemire, R.J., Berner, U., Musikas, C., Palmer, D.A., Taylor, P., Tochiyama, O., 2013.
1499 Chemical Thermodynamics 13a. Chemical Thermodynamics of Iron. Part 1. OECD
1500 Nuclear Energy Agency Data Bank, OECD Publications, Paris, France. http://www.oecd-
1501 nea.org/dbtdb/pubs/6355-vol13a-iron.pdf

1502 Lestini, L., Beaucaire, C., Vercouter, T., Ballini, M., Descostes, M., 2019. Role of trace
1503 elements in the 226-radium incorporation in sulfate minerals (gypsum and celestite).
1504 ACS Earth Space Chem. 3, 295-304.

1505 Li, B., Zhou, J.W., Priest, C., Jiang, D.E., 2017. Effect of salt on the uranyl binding with
1506 carbonate and calcium ions in aqueous solutions. J. Chem. Phys. B 121, 8171-8178.

1507 Lothenbach, B., Ochs, M., Wanner, H., Yui, M., 1999. Thermodynamic Data for the
1508 Speciation and Solubility of Pd, Pb, Sn, Sb, Nb, and Bi in Aqueous Solution. JNC, Ibaraki,
1509 Japan.
1510 http://www.iaea.org/inis/collection/NCLCollectionStore/_Public/31/009/31009694.p
1511 df

1512 Maher, K., Bargar, J.R., Brown, G.E., Jr., 2013. Environmental speciation of actinides.
1513 Inorg. Chem. 52, 3510-3532.

1514 Maloubier, M., Solari, P.L., Moisy, P., Monfort, M., Den Auwer, C., Moulin, C., 2015. XAS
1515 and TRLIF spectroscopy of uranium and neptunium in seawater. Dalton Trans. 44, 5417-
1516 5427.

1517 Martell, A.E., Smith, R.M., 1976. Critical Stability Constants. Volume 4: Inorganic
1518 Complexes. Plenum Press, New York, NY, USA.

1519 Martinez, J.S., Santillan, E.-F., Bossant, M., Costa, D., Ragoussi, M.-E., 2019. The new
1520 electronic database of the NEA Thermochemical Database Project. Appl. Geochem. 107,
1521 159-170.

1522 May, P.M., Filella, M., 2011. Chemical modelling of multicomponent mixtures: quality
1523 assurance is more than just equilibrium data quality assessment. Accredit. Qual. Assur.
1524 16, 179-184.

1525 MCPhreeqc, 2011. A tool for PHREEQC Monte-Carlo Simulations. Amphos 21.
1526 http://www.amphos21.com/vistas/descargas.php

Millero, F.J., Feistel, R., Wright, D.G., McDougall, T.J., 2008. The composition of Standard Seawater and the definition of the reference-composition salinity scale. Deep-Sea Res. Pt. I 55, 50-72.

Mitsakou, C., Eleftheriadis, K., Housiadas, C., Lazaridis, M., 2003. Modeling of the dispersion of depleted uranium aerosol. Health Phys. 84, 538-544.

Mompeán, F.J., Wanner, H., 2003. The OECD Nuclear Energy Agency Thermochemical Database Project. Radiochim. Acta 91, 617-621.

Montarnal, P., Mügler, C., Colin, J., Descostes, M., Dimier, A., Jacquot, E., 2007. Presentation and use of a reactive transport code in porous media. Physics and Chemistry of the Earth, Parts A/B/C 32, 507-517.

Mühr-Ebert, E.L., Wagner, F., Walther, C., 2019. Speciation of uranium: compilation of a thermodynamic database and its experimental evaluation using different analytical techniques. Appl. Geochem., 100, 213-222.

Murphy, R.J., Lenhart, J.J., Honeyman, B.D., 1999. The sorption of thorium (IV) and uranium (VI) to hematite in the presence of natural organic matter. Colloids Surf., A 157, 47-62.

Muto, T., 1965. Thermochemical stability of ningyoite. Mineral. J. 4, 245-274.

Neck, V., Kim, J.I., 2001. Solubility and hydrolysis of tetravalent actinides. Radiochim. Acta 89, 1-16.

Neiva, A.M.R., Carvalho, P.C.S., Antunes, I.M.H.R., Albuquerque, M.T.D., Santos, A.C.S., Cunha, P.P., Henriques, S.B.A., 2019. Assessment of metal and metalloid contamination in the waters and stream sediments around the abandoned uranium mine area from Mortórios, central Portugal. J. Geochem. Explor. 202, 35-48.

Nordstrom, D.K., 1996. Trace metal speciation in natural waters: computational vs. analytical. Water Air Soil Pollut. 90, 257-267.

Nordstrom, D.K., Plummer, L.N., Langmuir, D., Busenberg, E., May, H.M., Jones, B.F., Parkhurst, D.L., 1990. Revised chemical equilibrium data for major water-mineral reactions and their limitations. in: Melchior, D.C., Bassett, R.L. (Eds.). Chemical Modeling of Aqueous Systems II. American Chemical Society, Washington, DC, USA, pp. 398-413.

Nriagu, J.O., 1972a. Solubility equilibrium constant of strengite. Am. J. Sci. 272, 476-484.

Nriagu, J.O., 1972b. Stability of vivianite and ion-pair formation in the system $Fe_3(PO_4)_2$-H_3PO_4-H_2O. Geochim. Cosmochim. Acta 36, 459-470.

Nriagu, J.O., 1974. Lead orthophosphates—IV. Formation and stability in the environment. Geochim. Cosmochim. Acta 38, 887-898.

Nriagu, J.O., 1984. Formation and stability of base metal phosphates in soils and sediments. in: Nriagu, J.O., Moore, P.B. (Eds.). Phosphate Minerals. Springer Berlin Heidelberg, Berlin, Germany, pp. 318-329.

1564 O'Brien, T.J., Williams, P.A., 1983. The aqueous chemistry of uranium minerals. 4.
1565 Schröckingerite, grimselite, and related alkali uranyl carbonates. Mineral. Mag. 47, 69-
1566 73.

1567 Ödegaard-Jensen, A., Ekberg, C., Meinrath, G., 2004. LJUNGSKILE: a program for
1568 assessing uncertainties in speciation calculations. Talanta 63, 907-916.

1569 OECD, 2014. Uranium 2014: Resources, Production and Demand. OECD-IAEA, Paris,
1570 France, p. 504. http://www.oecd-nea.org/ndd/pubs/2014/7209-uranium-2014.pdf

1571 Olin, Å., Noläng, B., Osadchii, E.G., Öhman, L.-O., Rosén, E., 2005. Chemical
1572 Thermodynamics 7. Chemical Thermodynamics of Selenium. North Holland Elsevier
1573 Science Publishers B. V., Amsterdam, The Netherlands. http://www.oecd-
1574 nea.org/dbtdb/pubs/vol7-selenium.pdf

1575 Palmer, D.A., Wesolowski, D.J., 1997. Potentiometric measurements of the first
1576 hydrolysis quotient of magnesium(II) to 250°C and 5 molal ionic strength (NaCl). J. Solut.
1577 Chem. 26, 217-232.

1578 Pankratz, L.B., Mah, A.D., Watson, S.W., 1987. Thermodynamic Properties of Sulfides. U.S.
1579 Bureau of Mines Bulletin.
1580 http://digital.library.unt.edu/ark:/67531/metadc38801/m2/1/high_res_d/metadc388
1581 01.pdf

1582 Paredes, E., Avazeri, E., Malard, V., Vidaud, C., Reiller, P.E., Ortega, R., Nonell, A., Isnard,
1583 H., Chartier, F., Bresson, C., 2016. Evidence of isotopic fractionation of natural uranium
1584 in cultured human cells. P. Natl. Acad. Sci. USA 113, 14007-14012.

1585 Paredes, E., Avazeri, E., Malard, V., Vidaud, C., Reiller, P.E., Ortega, R., Nonell, A., Isnard,
1586 H., Chartier, F., Bresson, C., 2018. Impact of uranium uptake on isotopic fractionation and
1587 endogenous element homeostasis in human neuron-like cells. Sci. Rep. 8, 17163.

1588 Parkhurst, D.L., Appelo, C.A.J., 1999. User's Guide to PHREEQC (Version 2) — A
1589 Computer Program for Speciation, Batch-Reaction, One-Dimensional Transport, and
1590 Inverse Geochemical Calculations. U.S. Geological Survey, Water-Resources
1591 Investigations, Lakewood, Colorado, USA.
1592 http://wwwbrr.cr.usgs.gov/projects/GWC_coupled/phreeqci/

1593 Parkhurst, D.L., Appelo, C.A.J., 2013. Description of Input and Examples for PHREEQC
1594 Version 3 — A Computer Program for Speciation, Batch-Reaction, One-Dimensional
1595 Transport, and Inverse Geochemical Calculations. Chapter 43 of Section A, Groundwater
1596 Book 6, Modeling Techniques. U.S. Geological Survey, Denver, Colorado, USA, p. 497.
1597 http://pubs.usgs.gov/tm/06/a43/pdf/tm6-A43.pdf

1598 Plummer, L.N., Busenberg, E., 1982. The solubilities of calcite, aragonite and vaterite in
1599 CO_2-H_2O solutions between 0 and 90°C, and an evaluation of the aqueous model for the
1600 system $CaCO_3$-CO_2-H_2O. Geochim. Cosmochim. Acta 46, 1011-1040.

1601 Plyasunova, N.V., Wang, M.S., Zhang, Y., Muhammed, M., 1997. Critical evaluation of
1602 thermodynamics of complex formation of metal ions in aqueous solutions. II. Hydrolysis
1603 and hydroxo-complexes of Cu^{2+} at 298.15 K. Hydrometallurgy 45, 37-51.

1604 Powell, K.J., Brown, P.L., Byrne, R.H., Gajda, T., Hefter, G., Leuz, A.-K., Sjöberg, S., Wanner,
1605 H., 2013. Chemical speciation of environmentally significant metals with inorganic
1606 ligands. Part 5: The Zn^{2+} + OH^-, Cl^-, CO_3^{2-}, SO_4^{2-}, and PO_4^{3-} systems (IUPAC Technical
1607 Report). Pure Appl. Chem. 85, 2249-2311.

1608 Prat, O., Vercouter, T., Ansoborlo, E., Fichet, P., Perret, P., Kurttio, P., Salonen, L., 2009.
1609 Uranium speciation in drinking water from drilled wells in southern Finland and its
1610 potential links to health effects. Environ. Sci. Technol. 43, 3941-3946.

1611 Ragoussi, M.E., Brassinnes, S., 2015. The NEA Thermochemical Database Project: 30
1612 years of accomplishments. Radiochim. Acta 103, 679-685.

1613 Ramette, R.W., Sandford, R.W., Jr., 1965. Thermodynamics of iodine solubility and
1614 triiodide ion formation in water and in deuterium oxide. J. Am. Chem. Soc. 87, 5001-
1615 5005.

1616 Rand, M., Fuger, J., Grenthe, I., Neck, V., Rai, D., 2009. Chemical Thermodynamics 11.
1617 Chemical Thermodynamics of Thorium. OECD Nuclear Energy Agency Data Bank, OECD
1618 Publications, Paris, France. http://www.oecd-nea.org/science/pubs/2007/6254-DB-
1619 chemical-thermodyn-11.pdf

1620 Ranville, J.F., Hendry, M.J., Reszat, T.N., Xie, Q.L., Honeyman, B.D., 2007. Quantifying
1621 uranium complexation by groundwater dissolved organic carbon using asymmetrical
1622 flow field-flow fractionation. J. Contam. Hydrol. 91, 233-246.

1623 Reardon, E.J., 1983. Determination of $SrSO_4^0$ ion pair formation using conductimetric
1624 and ion exchange techniques. Geochim. Cosmochim. Acta 47, 1917-1922.

Reardon, E.J., Armstrong, D.K., 1987. Celestite ($SrSO_{4(S)}$) solubility in water, seawater and NaCl solution. Geochim. Cosmochim. Acta 51, 63-72.

Reiller, P.E., Marang, L., Jouvin, D., Benedetti, M.F., 2012. Uranium (VI) binding to humic substances: speciation, estimation of competition, and application to independant data. in: Merkel, B., Schipek, M. (Eds.). The New Uranium Mining Boom. Challenge and Lessons Learned. Springer-Verlag, Berlin, Germany, pp. 565-572.

Reinoso-Maset, E., Ly, J., 2016. Study of uranium(VI) and radium(II) sorption at trace level on kaolinite using a multisite ion exchange model. J. Environ. Radioactiv. 157, 136-148.

Robie, R.A., Hemingway, B.S., 1995. Thermodynamic Properties of Minerals and Related Substances at 298.15 K and 1 bar (10^5 Pascal) Pressure and at Higher Temperatures. US Geological Survey, Denver, CO, USA, p. 461. http://pubs.usgs.gov/bul/2131/report.pdf

Robin, V., Tertre, E., Beaucaire, C., Regnault, O., Descostes, M., 2017. Experimental data and assessment of predictive modeling for radium ion-exchange on beidellite, a swelling clay mineral with a tetrahedral charge. Appl. Geochem. 85, 1-9.

Sajih, M., Bryan, N.D., Livens, F.R., Vaughan, D.J., Descostes, M., Phrommavanh, V., Nos, J., Morris, K., 2014. Adsorption of radium and barium on goethite and ferrihydrite: a kinetic and surface complexation modelling study. Geochim. Cosmochim. Acta 146, 150-163.

Salas, J., Ayora, C., 2004. Groundwater chemistry of the Okelobondo uraninite deposit area (Oklo, Gabon): two-dimensional reactive transport modelling. J. Contam. Hydrol. 69, 115-137.

Shock, E.L., Sassani, D.C., Willis, M., Sverjensky, D.A., 1997. Inorganic species in geologic fluids: correlations among standard molal thermodynamic properties of aqueous ions and hydroxide complexes. Geochim. Cosmochim. Acta 61, 907-950.

Silva, R.J., Bidoglio, G., Rand, M., Robouch, P., Wanner, H., Puigdomènech, I., 1995. Chemical Thermodynamics 2. Chemical Thermodynamics of Americium with an Appendix on Chemical Thermodynamics of Uranium (Grenthe, I., Sandino, M. C. A., Puigdomènech, I., Rand, M. H., Eds.). North Holland Elsevier Science Publishers B. V., Amsterdam, The Netherlands. http://www.oecd-nea.org/dbtdb/pubs/americium.pdf

Siroux, B., Beaucaire, C., Tabarant, M., Benedetti, M.F., Reiller, P.E., 2017. Adsorption of strontium and caesium onto an Na-MX80 bentonite: experiments and building of a coherent thermodynamic modelling. Appl. Geochem. 87, 167-175.

Siroux, B., Wissocq, A., Beaucaire, C., Latrille, C., Petcut, C., Calvaire, J., Tabarant, M., Benedetti, M.F., Reiller, P.E., 2018. Adsorption of caesium and strontium onto an Na-illite and Na-illite/Na-smectite mixtures: application of a multi-site ion-exchanger model. Appl. Geochem. 99, 65-74.

Smith, R.M., Martell, A.E., Motekaitis, R.J., 2004. NIST Standard Reference Database 46. NIST critically selected stability constants of metal complexes database. Version 8.0. National Institute of Standards and Technology, Gaithersburg, MD, USA. http://www.nist.gov/srd/upload/46_8.htm

1665 Steefel, C.I., Appelo, C.A.J., Arora, B., Jacques, D., Kalbacher, T., Kolditz, O., Lagneau, V.,
1666 Lichtner, P.C., Mayer, K.U., Meeussen, J.C.L., Molins, S., Moulton, D., Shao, H., Simunek, J.,
1667 Spycher, N., Yabusaki, S.B., Yeh, G.T., 2015. Reactive transport codes for subsurface
1668 environmental simulation. Computat. Geosci. 19, 445-478.

1669 Stetten, L., Mangeret, A., Brest, J., Seder-Colomina, M., Le Pape, P., Ikogou, M., Zeyen, N.,
1670 Thouvenot, A., Julien, A., Alcalde, G., Reyss, J.L., Bombled, B., Rabouille, C., Olivi, L., Proux,
1671 O., Cazala, C., Morin, G., 2018. Geochemical control on the reduction of U(VI) to
1672 mononuclear U(IV) species in lacustrine sediments. Geochim. Cosmochim. Acta 222,
1673 171-186.

1674 Sverjensky, D.A., Shock, E.L., Helgeson, H.C., 1997. Prediction of the thermodynamic
1675 properties of aqueous metal complexes to 1000°C and 5 kb. Geochim. Cosmochim. Acta
1676 61, 1359-1412.

1677 Tagirov, B., Schott, J., 2001. Aluminum speciation in crustal fluids revisited. Geochim.
1678 Cosmochim. Acta 65, 3965-3992.

1679 Taylor, P., Lopata, V.J., 1984. Stability and solubility relationships between some solids in
1680 the system PbO-CO_2-H_2O. Can. J. Chem. 62, 395-402.

1681 Thoenen, T., Hummel, W., Berner, U., Curti, E., 2014. The PSI/Nagra Chemical
1682 Thermodynamic Database 12/07. Paul Scherrer Institute, Villigen, Switzerland, p. 416.
1683 http://www.psi.ch/les/database

Thury, M., Bossart, P., 1999. Mont-Terri Rock Laboratory. Results of the hydrogeological, geochemical and geotechnical experiments performed in 1996 and 1997. Swiss National Hydrological and Geological Survey, Bern, Switzerland, p. 234. http://www.mont-terri.ch/content/mont-terri-internet/en/documentation/publications-from-swisstopo.download/mont-terri-internet/en/publications/publications-swisstopo/GBD-23.pdf

van der Lee, J., De Windt, L., Lagneau, V., Goblet, P., 2003. Module-oriented modeling of reactive transport with HYTEC. Computers & Geosciences 29, 265-275.

Van Haverbeke, L., Vochten, R., Van Springel, K., 1996. Solubility and spectrochemical characteristics of synthetic chernikovite and meta-ankoleite. Mineral. Mag. 60, 759-766.

Vercouter, T., Reiller, P.E., Ansoborlo, E., Février, L., Gilbin, R., Lomenech, C., Philippini, V., 2015. A modelling exercise on the importance of ternary alkaline earth carbonate species of uranium(VI) in the inorganic speciation of natural waters. Appl. Geochem. 55, 192-198.

von Gunten, K., Warchola, T., Donner, M.W., Cossio, M., Hao, W., Boothman, C., Lloyd, J., Siddique, T., Partin, C.A., Flynn, S.L., Rosaasen, A., Konhauser, K.O., Alessi, D.S., 2018. Biogeochemistry of U, Ni, and As in two meromictic pit lakes at the Cluff Lake uranium mine, northern Saskatchewan. Can. J. Earth Sci. 55, 463-474.

Wagman, D.D., Evans, W.H., Parker, V.B., Schumm, R.H., Halow, I., Bailey, S.M., Churney, K.L., Nuttall, R.L., 1982. The NBS Tables of chemical thermodynamic properties. Selected values for inorganic and C_1 and C_2 organic substances in SI units. J. Chem. Ref. Data 11, 392.

Waite, T.D., Davis, J.A., Payne, T.E., Waychunas, G.A., Xu, N., 1994. Uranium(VI) adsorption to ferrihydrite: application of a surface complexation model. Geochim. Cosmochim. Acta 58, 5465-5478.

Wang, M., Zhang, Y., Muhammed, M., 1997. Critical evaluation of thermodynamics of complex formation of metal ions in aqueous solutions III. The system Cu(I,II) $-Cl^-$ $-e$ at 298.15 K. Hydrometallurgy 45, 53-72.

Wang, X., Shi, Z., Kinniburgh, D.G., Zhao, L., Ni, S., Wang, R., Hou, Y., Cheng, K., Zhu, B., 2019. Effect of thermodynamic database selection on the estimated aqueous uranium speciation. J. Geochem. Explor. 204, 33-42.

Wanner, H., 1988. The NEA thermochemical data-base project. Radiochim. Acta 44-45, 325-329.

Wieser, M.E., 2006. Atomic weight of the elements 2005 (IUPAC technical report). Pure Appl. Chem. 78, 2051-2066.

Wissocq, A., Beaucaire, C., Latrille, C., 2018. Application of the multi-site ion exchanger model to the sorption of Sr and Cs on natural clayey sandstone. Appl. Geochem. 93, 167.177.

1722 Yabusaki, S.B., Fang, Y., Long, P.E., Resch, C.T., Peacock, A.D., Komlos, J., Jaffe, P.R.,
1723 Morrison, S.J., Dayvault, R.D., White, D.C., Anderson, R.T., 2007. Uranium removal from
1724 groundwater via in situ biostimulation: field-scale modeling of transport and biological
1725 processes. J. Contam. Hydrol. 93, 216-235.

1726 Yeatts, L.B., Marshall, W.L., 1969. Apparent invariance of activity coefficients of calcium
1727 sulfate at constant ionic strength and temperature in system $CaSO_4$-Na_2SO_4-$NaNO_3$-H_2O
1728 to critical temperature of water. Association equilibria. J. Phys. Chem. 73, 81-90.

1729 Zhang, Y., Muhammed, M., 2001. Critical evaluation of thermodynamics of complex
1730 formation of metal ions in aqueous solutions: VI. Hydrolysis and hydroxo-complexes of
1731 Zn^{2+} at 298.15 K. Hydrometallurgy 60, 215-236.

1732 Zhu, C., Hu, F.Q., Burden, D.S., 2001. Multi-component reactive transport modeling of
1733 natural attenuation of an acid groundwater plume at a uranium mill tailings site. J.
1734 Contam. Hydrol. 52, 85-108.

1735